

Further analysis of the budgets of the dissipation tensor ε_{ij} in turbulent plane channel flow

G. A. Gerolymos and I. Vallet

Sorbonne Universités, Université Pierre-et-Marie-Curie, 4 place Jussieu, 75005 Paris, France

E-mail: georges.gerolymos@upmc.fr and isabelle.vallet@upmc.fr

Abstract. Recent DNS results [Gerolymos G.A., Vallet I. : *J. Fluid Mech.* **807** (2016) 386–418] have provided data for the terms in the transport equations for the components of the dissipation tensor ε_{ij} in low-Reynolds turbulent plane channel flow. The present paper extends the previous results by a detailed analysis of the behaviour of various mechanisms in the ε_{ij} -transport equations (production, diffusion, redistribution, destruction), with particular emphasis on the component-by-component comparison with the corresponding mechanisms in the transport equations for the Reynolds-stresses r_{ij} . The splitting of the pressure terms for the wall-normal components into redistribution and pressure-diffusion reveals substantially different behaviour near the wall. The wall-asymptotics of different terms in the transport equations are studied in detail, and examined using the DNS data. Both DNS data and wall-asymptotic analysis show that the anisotropy of the destruction-of-dissipation tensor $\varepsilon_{\varepsilon_{ij}}$ is fundamentally different from that of r_{ij} or ε_{ij} , never approaching the 2-component (2-C) state at the solid wall.

1. Introduction

Transport equations (Chou, 1945) of 1-point and 2-point statistics are essential both in understanding turbulence dynamics (Tennekes and Lumley, 1972) and in providing the theoretical foundations for turbulence modelling (Schiestel, 2008). The fluctuating-velocity-covariance (2-moment) tensor $r_{ij} := \overline{u'_i u'_j}$, which defines the Reynolds-stresses $-\rho r_{ij}$, is governed by well known transport equations (Mansour, Kim and Moin, 1988, (1), p. 17) where the dissipation tensor ε_{ij} represents the destruction of r_{ij} by molecular friction (viscosity). The dissipation tensor ε_{ij} also follows transport equations (Gerolymos and Vallet, 2016a, (3.3), p. 403) where the destruction-of-dissipation tensor $\varepsilon_{\varepsilon_{ij}}$ represents the destruction of ε_{ij} by molecular viscosity. Of course $\varepsilon_{\varepsilon_{ij}}$ is governed in turn by its own transport equation where appears its own destruction-rate, and so on to correlations of higher derivatives of the fluctuating velocity.

The budgets of the r_{ij} -transport equations (1a) have been studied extensively using DNS (Mansour et al., 1988; Moser, Kim and Mansour, 1999; Sillero, Jiménez and Moser, 2013). Closure of noncomputable terms in (1a), along with a transport equation for some scalar scale-determining variable (Jones and Launder, 1972; Launder and Spalding, 1974; Wilcox, 1988; Menter, 1994; Jakirlić and Hanjalić, 2002) has led (Launder, Reece and Rodi, 1975) to the development of second-moment

closures (SMCs) or Reynolds-stress models (RSMs). Several models of this family have been assessed for the computation of complex 3-D flows (Gerolymos and Vallet, 2001; Jakirlić, Einfeld, Jester-Zürker and Kroll, 2007; Cécora, Radespiel, Einfeld and Probst, 2015) and are increasingly used to predict practical 3-D configurations (Einfeld, 2015). Comparisons with measurements (Rumsey, 2010) demonstrate the predictive improvement of 7-equation RSMs against standard 2-equation approaches, especially in presence of separation and/or secondary flows (Gerolymos, Joly, Mallet and Vallet, 2010; Gerolymos and Vallet, 2016b) but also highlight remaining challenges. In general RSMs cannot return the correct wall-asymptotic behaviour for all of the components of the Reynolds-stress tensor (Yakovenko and Chang, 2007), and privileging the wall-normal components improves log-law prediction (Gerolymos, Lo, Vallet and Younis, 2012). An even more difficult challenge is to correctly mimic the Re -dependence of the near-wall maxima of the diagonal Reynolds-stresses which is revealed by DNS results (Lee and Moser, 2015). Finally, the hysteretic behaviour of the separation-and-reattachment process (Gerolymos, Kallas and Papailiou, 1989) may require additional specific lag-treatments (Olsen and Coakley, 2001).

The correct prediction of near-wall anisotropy (Durbin, 1993) and of lengthscale anisotropy in general (Lumley, Yang and Shih, 1999) is necessary to meet these challenges. The replacement of the scalar scale-determining equation used in classical RSMs (Wilcox, 2006; Schiestel, 2008) by transport equations for the individual components of ε_{ij} has been suggested to overcome the unsatisfactory *a posteriori* performance of algebraic ε_{ij} -closures (Gerolymos, Lo, Vallet and Younis, 2012). Detailed DNS data of the ε_{ij} -transport equations (1b) are necessary to achieve this goal.

Scrutiny of the budgets of the scalar ε -equation ($\varepsilon := \frac{1}{2}\varepsilon_{mm}$) provided by DNS (Mansour et al., 1988) has proved particularly useful in improving the closure of this equation (Lai and So, 1990; Rodi and Mansour, 1993; Jakirlić and Hanjalić, 2002). On the other hand, very little work has been done concerning the budgets of the tensorial ε_{ij} -equations (1b). In a recent work (Gerolymos and Vallet, 2016a) we have generated DNS data of ε_{ij} -budgets for low- Re turbulent plane channel flow and discussed the behaviour of various terms in (1b), with particular emphasis on the 4 production mechanisms.

The purpose of the present work is to further analyze ε_{ij} -budgets in turbulent plane channel flow, and in particular the similarities and differences with respect to r_{ij} -budgets. In §2 we define the terms in the transport equations for r_{ij} and ε_{ij} , and calculate the wall-asymptotic behaviour of different terms in the ε_{ij} -transport equations (1b) for the particular case of turbulent plane channel flow. These analytical results are used (§3) to assess very-near-wall DNS data. In §3 we use DNS data (§3.1) to compare r_{ij} -budgets with ε_{ij} -budgets (§3.2) and to analyze the splitting of the pressure term $\Pi_{\varepsilon_{ij}}$ in (1b) into a redistributive and a conservative term (§3.3). In §4 we compare the anisotropy and associated anisotropy invariant mapping (AIM) of the Reynolds-stresses r_{ij} , their dissipation ε_{ij} and the destruction-of-dissipation $\varepsilon_{\varepsilon_{ij}}$ which exhibits a notably different componentality near the wall. Finally, in §5, we summarize the main results of the present work.

2. Transport equations and wall asymptotics

Consistent with the DNS data, we study incompressible flow with a Newtonian constitutive relation in an inertial frame (Gerolymos and Vallet, 2016a). We use

a Cartesian reference-frame $x_i \in \{x, y, z\}$, note $u_i \in \{u, v, w\}$ the corresponding components of the velocity vector, and use Reynolds decomposition into averaged $\overline{(\cdot)}$ and fluctuating $(\cdot)'$ quantities, We note t the time, $\rho \cong \text{const}$ the density, p the pressure, $\nu \cong \text{const}$ the kinematic viscosity, and $\mu := \rho\nu \cong \text{const}$ the dynamic viscosity.

2.1. Transport equations

Straightforward manipulations of the fluctuating momentum (B.7) and of the fluctuating continuity (B.3) equations and of their gradients lead to the transport equations for $r_{ij} := \overline{u'_i u'_j}$ (Mansour et al., 1988, (1), p. 17)

$$\underbrace{\rho \frac{\partial \overline{u'_i u'_j}}{\partial t} + \rho \bar{u}_\ell \frac{\partial \overline{u'_i u'_j}}{\partial x_\ell}}_{C_{ij}} = \underbrace{\frac{\partial}{\partial x_\ell} \left(\mu \frac{\partial \overline{u'_i u'_j}}{\partial x_\ell} \right)}_{d_{ij}^{(\mu)}} + \underbrace{\frac{\partial}{\partial x_\ell} \left(-\rho \overline{u'_i u'_j u'_\ell} \right)}_{d_{ij}^{(u)}} + \underbrace{\left(-\overline{u'_i \frac{\partial p'}{\partial x_j}} - \overline{u'_j \frac{\partial p'}{\partial x_i}} \right)}_{\Pi_{ij}} + \underbrace{\left(-\rho \overline{u'_i u'_\ell} \frac{\partial \bar{u}_j}{\partial x_\ell} - \rho \overline{u'_j u'_\ell} \frac{\partial \bar{u}_i}{\partial x_\ell} \right)}_{P_{ij}} - \underbrace{\left(2\mu \frac{\partial \overline{u'_i}}{\partial x_\ell} \frac{\partial \overline{u'_j}}{\partial x_\ell} \right)}_{\rho \varepsilon_{ij}} \quad (1a)$$

and ε_{ij} (Gerolymos and Vallet, 2016a, (3.3), p. 403)

$$\begin{aligned} \underbrace{\rho \frac{\partial \varepsilon_{ij}}{\partial t} + \rho \bar{u}_\ell \frac{\partial \varepsilon_{ij}}{\partial x_\ell}}_{C_{\varepsilon_{ij}}} &= \underbrace{\frac{\partial}{\partial x_\ell} \left[\mu \frac{\partial \varepsilon_{ij}}{\partial x_\ell} \right]}_{d_{\varepsilon_{ij}}^{(\mu)}} + \underbrace{\frac{\partial}{\partial x_\ell} \left[-\rho \left(\overline{u'_\ell 2\nu \frac{\partial u'_i}{\partial x_k} \frac{\partial u'_j}{\partial x_k}} \right) \right]}_{d_{\varepsilon_{ij}}^{(u)}} \\ &\quad - \underbrace{\rho \varepsilon_{i\ell} \frac{\partial \bar{u}_j}{\partial x_\ell} - \rho \varepsilon_{j\ell} \frac{\partial \bar{u}_i}{\partial x_\ell}}_{P_{\varepsilon_{ij}}^{(1)}} - \underbrace{\rho \left(2\nu \frac{\partial \overline{u'_i}}{\partial x_k} \frac{\partial \overline{u'_j}}{\partial x_\ell} \right) \left(\frac{\partial \bar{u}_k}{\partial x_\ell} + \frac{\partial \bar{u}_\ell}{\partial x_k} \right)}_{P_{\varepsilon_{ij}}^{(2)}} \\ &\quad - \underbrace{\rho \left(2\nu \overline{u'_\ell} \frac{\partial \overline{u'_i}}{\partial x_k} \right) \frac{\partial^2 \bar{u}_j}{\partial x_\ell \partial x_k} - \rho \left(2\nu \overline{u'_\ell} \frac{\partial \overline{u'_j}}{\partial x_k} \right) \frac{\partial^2 \bar{u}_i}{\partial x_\ell \partial x_k}}_{P_{\varepsilon_{ij}}^{(3)}} - \underbrace{\rho \left[2\nu \frac{\partial \overline{u'_\ell}}{\partial x_k} \left(\frac{\partial \overline{u'_i}}{\partial x_k} \frac{\partial \overline{u'_j}}{\partial x_\ell} + \frac{\partial \overline{u'_j}}{\partial x_k} \frac{\partial \overline{u'_i}}{\partial x_\ell} \right) \right]}_{\Xi_{\varepsilon_{ij}} =: P_{\varepsilon_{ij}}^{(4)}} \\ &\quad - \underbrace{2\nu \frac{\partial \overline{u'_i}}{\partial x_k} \frac{\partial^2 \bar{p}'}{\partial x_j \partial x_k} - 2\nu \frac{\partial \overline{u'_j}}{\partial x_k} \frac{\partial^2 \bar{p}'}{\partial x_i \partial x_k}}_{\Pi_{\varepsilon_{ij}}} - \underbrace{\rho \left(2\nu \frac{\partial^2 \overline{u'_i}}{\partial x_k \partial x_\ell} \right) \left(2\nu \frac{\partial^2 \overline{u'_j}}{\partial x_k \partial x_\ell} \right)}_{\rho \varepsilon_{\varepsilon_{ij}}} \end{aligned} \quad (1b)$$

which were reproduced here for completeness.

The common origin of (1a, 1b) leads to analogous mechanisms in both transport equations, where convection by the mean flow ($C_{ij}, C_{\varepsilon_{ij}}$) is balanced by 5 mechanisms: diffusion by molecular viscosity ($d_{ij}^{(\mu)}, d_{\varepsilon_{ij}}^{(\mu)}$), turbulent diffusion (mixing) by the fluctuating velocity field u'_ℓ ($d_{ij}^{(u)}, d_{\varepsilon_{ij}}^{(u)}$), production by various mechanisms ($P_{ij}, P_{\varepsilon_{ij}} := P_{\varepsilon_{ij}}^{(1)} + P_{\varepsilon_{ij}}^{(2)} + P_{\varepsilon_{ij}}^{(3)} + P_{\varepsilon_{ij}}^{(4)}$), the fluctuating-pressure mechanisms ($\Pi_{ij}, \Pi_{\varepsilon_{ij}}$), and destruction by molecular viscosity ($\varepsilon_{ij}, \varepsilon_{\varepsilon_{ij}}$). Of course the tensorial componentality

(Lumley, 1978; Kassinos, Reynolds and Rogers, 2001; Simonsen and Krogstad, 2005) and the scaling (Tennekes and Lumley, 1972, pp. 88–92) of various terms in (1b) differs from that of the corresponding terms in (1a).

2.2. Wall asymptotics

Before studying the present DNS data for the ε_{ij} -transport budgets (3.2), it is useful to summarize the theoretically expected (Appendix B) asymptotic behaviour of various terms in the viscous sublayer, or, formally, as $y^+ \rightarrow 0$. Inner scaling (Buschmann and Gad-el-Hak, 2007, \cdot^+) is consistently used in these calculations (Appendix B). Wall-asymptotics of the terms in (1b) which only involve fluctuating velocities and their derivatives ($d_{\varepsilon_{ij}}^{(\mu)}$, $d_{\varepsilon_{ij}}^{(u)}$, $P_{\varepsilon_{ij}}^{(4)}$, $\varepsilon_{\varepsilon_{ij}}$) can be readily obtained from the Taylor-series expansions (Riley, Hobson and Bence, 2006, §4.6, pp. 136–141) of $u_i'^+$ in the wall-normal direction y^+

$$\begin{aligned} (\cdot)^+ \underset{y^+ \rightarrow 0}{\sim} & (\cdot)'_w(x^+, z^+, t^+) + A'_{(\cdot)}(x^+, z^+, t^+) y^+ + B'_{(\cdot)}(x^+, z^+, t^+) y^{+2} \\ & + C'_{(\cdot)}(x^+, z^+, t^+) y^{+3} + D'_{(\cdot)}(x^+, z^+, t^+) y^{+4} + \dots \end{aligned} \quad (2)$$

under the constraints of the no-slip condition at the wall (A.1a) and of the fluctuating continuity equation (§B.1). On the contrary, determination of the wall-asymptotics of terms in (1b) which contain the fluctuating pressure and its derivatives ($\Pi_{\varepsilon_{ij}}$) or the mean-flow velocities and their derivatives ($C_{\varepsilon_{ij}}$, $P_{\varepsilon_{ij}}^{(1)}$, $P_{\varepsilon_{ij}}^{(2)}$, $P_{\varepsilon_{ij}}^{(3)}$), requires specific simplifications implied by the fully developed plane channel flow conditions (A.1–A.3), in line with the analysis of the budgets of r_{ij} and ε in Mansour et al. (1988). Using (2, B.4, B.5), along with specific results (B.6–B.12) applicable to plane channel flow satisfying conditions (A.1–A.3), readily yields the wall-asymptotic expansions (Tabs. 1, 2) of various terms in the ε_{ij} -transport equations (1b). The homogeneity relations (A.3) were used, when applicable to simplify these expressions. The plane channel flow identity $\overline{B_u^+ C_v'^+} \stackrel{(B.11c)}{=} 0$ was used in $\varepsilon_{\varepsilon_{ij}}^+$, $d_{\varepsilon_{xy}}^{(\mu)+}$ and $\Pi_{\varepsilon_{xy}}^+$ (Tab. 1), while the plane channel flow identity (B.12) was used to replace $\overline{B_v' \partial_t A_u^+}$ in $\Pi_{\varepsilon_{xy}}^+$ (Tab. 1). These results (Tabs. 1, 2) are used in the analysis of the DNS data (§3).

3. Turbulent plane channel flow budgets

DNS data generated for plane channel flow (§3.1) illustrate how corresponding mechanisms in the transport equations of r_{ij} (1a) or ε_{ij} (1b) contribute to the budgets of different components (§3.2). In direct analogy to r_{ij} -transport (Mansour et al., 1988), the fluctuating-pressure mechanisms in ε_{ij} -transport (1b), $\Pi_{\varepsilon_{ij}}$, can be analysed (§3.3) as the sum of a traceless redistributive term $\phi_{\varepsilon_{ij}}$ and a conservative pressure-diffusion part $d_{\varepsilon_{ij}}^{(u)}$.

3.1. DNS computations

The DNS computations from which the present data were extracted are described in Gerolymos and Vallet (2016a). They were obtained for low $Re_{\tau_w} \approx 180$ plane channel flow using a very-high-order (Gerolymos, S  n  chal and Vallet, 2009) finite-volume solver (Gerolymos, S  n  chal and Vallet, 2010) which has been thoroughly validated

$$\begin{aligned}
d_{\varepsilon_{xx}}^{(\mu)+} &\sim 4 \left(\overline{6A_u'^+ C_u'^+} + \overline{4B_u'^+{}^2} + \overline{(\nabla A_u')^+{}^2} \right) \\
&\quad + 24 \left(\overline{4A_u'^+ D_u'^+} + \overline{6B_u'^+ C_u'^+} + \overline{(\nabla A_u')^+ \cdot (\nabla B_u')^+} \right) y^+ + O(y^{+2}) \\
d_{\varepsilon_{xy}}^{(\mu)+} &\sim 4 \left(\overline{3A_u'^+ C_v'^+} + \overline{4B_u'^+ B_v'^+} \right) \\
&\quad + 12 \left(\overline{4A_u'^+ D_v'^+} + \overline{6B_v'^+ C_u'^+} + \overline{(\nabla A_u')^+ \cdot (\nabla B_v')^+} \right) y^+ + O(y^{+2}) \\
d_{\varepsilon_{yy}}^{(\mu)+} &\sim 16 \overline{B_v'^+{}^2} + 144 \overline{B_v'^+ C_v'^+} y^+ + O(y^{+2}) \\
d_{\varepsilon_{zz}}^{(\mu)+} &\sim 4 \left(\overline{6A_w'^+ C_w'^+} + \overline{4B_w'^+{}^2} + \overline{(\nabla A_w')^+{}^2} \right) \\
&\quad + 24 \left(\overline{4A_w'^+ D_w'^+} + \overline{6B_w'^+ C_w'^+} + \overline{(\nabla A_w')^+ \cdot (\nabla B_w')^+} \right) y^+ + O(y^{+2}) \\
d_{\varepsilon_{xx}}^{(u)+} &\sim -4 \overline{A_u'^+{}^2 B_v'^+} y^+ - 6 \left(\overline{A_u'^+{}^2 C_v'^+} + \overline{4A_u'^+ B_u'^+ B_v'^+} \right) y^{+2} + O(y^{+3}) \\
d_{\varepsilon_{xy}}^{(u)+} &\sim -12 \overline{A_u'^+ B_v'^+{}^2} y^{+2} - \left(\overline{40A_u'^+ B_v'^+ C_v'^+} + \overline{32B_u'^+ B_v'^+{}^2} \right) y^{+3} + O(y^{+4}) \\
d_{\varepsilon_{yy}}^{(u)+} &\sim -32 \overline{B_v'^+{}^3} y^{+3} - 160 \overline{B_v'^+{}^2 C_v'^+} y^{+4} + O(y^{+5}) \\
d_{\varepsilon_{zz}}^{(u)+} &\sim -4 \overline{A_w'^+{}^2 B_v'^+} y^+ - 6 \left(\overline{A_w'^+{}^2 C_v'^+} + \overline{4A_w'^+ B_v'^+ B_w'^+} \right) y^{+2} + O(y^{+3}) \\
\Pi_{\varepsilon_{xx}}^+ &\sim 8 \overline{B_v'^+ \frac{\partial A_u'^+}{\partial x^+}} + 8 \left(\overline{3C_v'^+ \frac{\partial A_u'^+}{\partial x^+}} + \overline{2B_v'^+ \frac{\partial B_u'^+}{\partial x^+}} - \overline{(\nabla A_u')^+ \cdot (\nabla B_u')^+} \right) y^+ + O(y^{+2}) \\
\Pi_{\varepsilon_{xy}}^+ &\sim -12 \overline{A_u'^+ C_v'^+} - 4 \left(\overline{12A_u'^+ D_v'^+} + \overline{6B_v'^+ C_u'^+} - \overline{(\nabla A_u')^+ \cdot (\nabla B_v')^+} \right) y^+ + O(y^{+2}) \\
\Pi_{\varepsilon_{yy}}^+ &\sim -48 \overline{B_v'^+ C_v'^+} y^+ + 8 \left(\overline{-24B_v'^+ D_v'^+} - \overline{9C_v'^+{}^2} + \overline{(\nabla B_v')^+{}^2} \right) y^{+2} + O(y^{+3}) \\
\Pi_{\varepsilon_{zz}}^+ &\sim 8 \overline{B_v'^+ \frac{\partial A_w'^+}{\partial z^+}} + 8 \left(\overline{3C_v'^+ \frac{\partial A_w'^+}{\partial z^+}} + \overline{2B_v'^+ \frac{\partial B_w'^+}{\partial z^+}} - \overline{(\nabla A_w')^+ \cdot (\nabla B_w')^+} \right) y^+ + O(y^{+2}) \\
d_{\varepsilon_{xx}}^{(p)+} &= d_{\varepsilon_{zz}}^{(p)+} = 0 \quad \forall y^+ \\
d_{\varepsilon_{xy}}^{(p)+} &\sim -8 \left(\overline{B_u'^+ B_v'^+} + \overline{3A_u'^+ C_v'^+} \right) - 48 \left(\overline{A_u'^+ D_v'^+} + \overline{B_v'^+ C_u'^+} \right) y^+ + O(y^{+2}) \\
d_{\varepsilon_{yy}}^{(p)+} &\sim -16 \overline{B_v'^+{}^2} - 192 \overline{B_v'^+ C_v'^+} y^+ - 8 \left(\overline{48B_v'^+ D_v'^+} + \overline{36C_v'^+{}^2} \right) y^{+2} + O(y^{+3}) \\
\phi_{\varepsilon_{xx}}^+ &= \Pi_{\varepsilon_{xx}}^+ \quad \forall y^+ \\
\phi_{\varepsilon_{xy}}^+ &\sim \left(\overline{8B_u'^+ B_v'^+} + \overline{12A_u'^+ C_v'^+} \right) + 4 \left(\overline{6B_v'^+ C_u'^+} + \overline{(\nabla A_u')^+ \cdot (\nabla B_v')^+} \right) y^+ + O(y^{+2}) \\
\phi_{\varepsilon_{yy}}^+ &\sim 16 \overline{B_v'^+{}^2} + 144 \overline{B_v'^+ C_v'^+} y^+ + 8 \left(\overline{24B_v'^+ D_v'^+} + \overline{27C_v'^+{}^2} + \overline{(\nabla B_v')^+{}^2} \right) y^{+2} + O(y^{+3}) \\
\phi_{\varepsilon_{zz}}^+ &= \Pi_{\varepsilon_{zz}}^+ \quad \forall y^+
\end{aligned}$$

Table 1. Asymptotic (as $y^+ \rightarrow 0$) expansions (2) of various terms ($d_{\varepsilon_{ij}}^{(\mu)}$, $d_{\varepsilon_{ij}}^{(u)}$, $d_{\varepsilon_{ij}}^{(p)}$, $\phi_{\varepsilon_{ij}}$, $\Pi_{\varepsilon_{ij}}$) in the ε_{ij} -transport equations (1b), in wall-units (Gerolymos and Vallet, 2016a, (A3), p. 414), for the particular case of plane channel flow (A.1–A.3).

$$\begin{aligned}
\varepsilon_{\varepsilon_{xx}}^+ &\sim 8 \left(2 \overline{B_u'^+{}^2} + \overline{(\nabla A_u')^+{}^2} \right) + 32 \left(3 \overline{B_u'^+ C_u'^+} + \overline{(\nabla A_u')^+ \cdot (\nabla B_u')^+} \right) y^+ + O(y^{+2}) \\
\varepsilon_{\varepsilon_{xy}}^+ &\sim 16 \overline{B_u'^+ B_v'^+} + 16 \left(3 \overline{B_v'^+ C_u'^+} + \overline{(\nabla A_u')^+ \cdot (\nabla B_v')^+} \right) y^+ + O(y^{+2}) \\
\varepsilon_{\varepsilon_{yy}}^+ &\sim 16 \overline{B_v'^+{}^2} + 96 \overline{B_v'^+ C_v'^+} y^+ + O(y^{+2}) \\
\varepsilon_{\varepsilon_{zz}}^+ &\sim 8 \left(2 \overline{B_w'^+{}^2} + \overline{(\nabla A_w')^+{}^2} \right) + 32 \left(3 \overline{B_w'^+ C_w'^+} + \overline{(\nabla A_w')^+ \cdot (\nabla B_w')^+} \right) y^+ + O(y^{+2}) \\
P_{\varepsilon_{xx}}^{(1)+} &\sim -8 \overline{A_u'^+ B_v'^+} y^+ + \left(\frac{8 \overline{A_u'^+ B_v'^+}}{Re_{\tau_w}} - 12 \overline{A_u'^+ C_v'^+} - 16 \overline{B_u'^+ B_v'^+} \right) y^{+2} + O(y^{+3}) \\
P_{\varepsilon_{xy}}^{(1)+} &\sim -8 \overline{B_v'^+{}^2} y^{+2} + 8 \left(\frac{\overline{B_v'^+{}^2}}{Re_{\tau_w}} - 3 \overline{B_v'^+ C_v'^+} \right) y^{+3} + O(y^{+4}) \\
P_{\varepsilon_{yy}}^{(1)+} &= P_{\varepsilon_{zz}}^{(1)+} = 0 \quad \forall y^+ \\
P_{\varepsilon_{xx}}^{(2)+} &\sim -4 \overline{B_u'^+ \frac{\partial A_u'^+}{\partial x^+}} y^{+2} - 4 \left(2 \overline{C_u'^+ \frac{\partial A_u'^+}{\partial x^+}} - \frac{1}{Re_{\tau_w}} \overline{B_u'^+ \frac{\partial A_u'^+}{\partial x^+}} \right) y^{+3} + O(y^{+4}) \\
P_{\varepsilon_{xy}}^{(2)+} &\sim -2 \overline{B_v'^+ \frac{\partial A_u'^+}{\partial x^+}} y^{+2} - 2 \left(2 \overline{C_v'^+ \frac{\partial A_u'^+}{\partial x^+}} - \frac{1}{Re_{\tau_w}} \overline{B_v'^+ \frac{\partial A_u'^+}{\partial x^+}} \right) y^{+3} + O(y^{+4}) \\
P_{\varepsilon_{yy}}^{(2)+} &\sim -4 \overline{C_v'^+ \frac{\partial B_v'^+}{\partial x^+}} y^{+4} - 4 \left(2 \overline{D_v'^+ \frac{\partial B_v'^+}{\partial x^+}} - \frac{1}{Re_{\tau_w}} \overline{C_v'^+ \frac{\partial B_v'^+}{\partial x^+}} \right) y^{+5} + O(y^{+6}) \\
P_{\varepsilon_{zz}}^{(2)+} &\sim -4 \overline{B_w'^+ \frac{\partial A_w'^+}{\partial x^+}} y^{+2} - 4 \left(2 \overline{C_w'^+ \frac{\partial A_w'^+}{\partial x^+}} - \frac{1}{Re_{\tau_w}} \overline{B_w'^+ \frac{\partial A_w'^+}{\partial x^+}} \right) y^{+3} + O(y^{+4}) \\
P_{\varepsilon_{xx}}^{(3)+} &\sim \frac{4}{Re_{\tau_w}} \overline{A_u'^+ B_v'^+} y^{+2} + \frac{4}{Re_{\tau_w}} \left(\overline{A_u'^+ C_v'^+} + 2 \overline{B_u'^+ B_v'^+} \right) y^{+3} + O(y^{+4}) \\
P_{\varepsilon_{xy}}^{(3)+} &\sim \frac{4}{Re_{\tau_w}} \overline{B_v'^+{}^2} y^{+3} + \frac{10}{Re_{\tau_w}} \overline{B_v'^+ C_v'^+} y^{+4} + O(y^{+5}) \\
P_{\varepsilon_{yy}}^{(3)+} &= P_{\varepsilon_{zz}}^{(3)+} = 0 \quad \forall y^+ \\
P_{\varepsilon_{xx}}^{(4)+} &\sim -12 \overline{A_u'^+{}^2 B_v'^+} y^+ - 4 \left(6 \overline{A_u'^+{}^2 C_v'^+} + 8 \overline{A_u'^+ B_u'^+ B_v'^+} - \overline{A_u'^+ B_u'^+ \frac{\partial A_w'^+}{\partial z^+}} + \overline{A_w'^+ B_u'^+ \frac{\partial A_u'^+}{\partial z^+}} \right) y^{+2} \\
&\quad + O(y^{+3}) \\
P_{\varepsilon_{xy}}^{(4)+} &\sim -2 \left(8 \overline{A_u'^+ B_v'^+{}^2} - \overline{A_u'^+ B_v'^+ \frac{\partial A_w'^+}{\partial z^+}} + \overline{A_w'^+ B_v'^+ \frac{\partial A_u'^+}{\partial z^+}} \right) y^{+2} \\
&\quad - 4 \left(16 \overline{A_u'^+ B_v'^+ C_v'^+} + 8 \overline{B_u'^+ B_v'^+{}^2} - \overline{B_u'^+ B_v'^+ \frac{\partial A_w'^+}{\partial z^+}} + \overline{B_w'^+ B_v'^+ \frac{\partial A_u'^+}{\partial z^+}} + \overline{A_w'^+ C_v'^+ \frac{\partial A_u'^+}{\partial z^+}} + \overline{A_u'^+ C_v'^+ \frac{\partial A_w'^+}{\partial x^+}} \right) y^{+3} \\
&\quad + O(y^{+4}) \\
P_{\varepsilon_{yy}}^{(4)+} &\sim -40 \overline{B_v'^+{}^3} y^{+3} - 4 \left(46 \overline{B_v'^+{}^2 C_v'^+} + \overline{A_u'^+ C_v'^+ \frac{\partial B_v'^+}{\partial x^+}} + \overline{A_w'^+ C_v'^+ \frac{\partial B_v'^+}{\partial z^+}} \right) y^{+4} + O(y^{+5}) \\
P_{\varepsilon_{zz}}^{(4)+} &\sim -12 \overline{A_w'^+{}^2 B_v'^+} y^+ - 4 \left(6 \overline{A_w'^+{}^2 C_v'^+} + 8 \overline{A_w'^+ B_w'^+ B_v'^+} - \overline{A_w'^+ B_w'^+ \frac{\partial A_u'^+}{\partial x^+}} + \overline{A_u'^+ B_w'^+ \frac{\partial A_w'^+}{\partial x^+}} \right) y^{+2} \\
&\quad + O(y^{+3})
\end{aligned}$$

Table 2. Asymptotic (as $y^+ \rightarrow 0$) expansions (2) of the various mechanisms of production $P_{\varepsilon_{ij}} = P_{\varepsilon_{ij}}^{(1)} + P_{\varepsilon_{ij}}^{(2)} + P_{\varepsilon_{ij}}^{(3)} + P_{\varepsilon_{ij}}^{(4)}$ and of the destruction-of-dissipation $\varepsilon_{\varepsilon_{ij}}$ appearing in the ε_{ij} -transport equations (1b), in wall-units (Gerolymos and Vallet, 2016a, (A3), p. 414), for the particular case of plane channel flow (A.1–A.3).

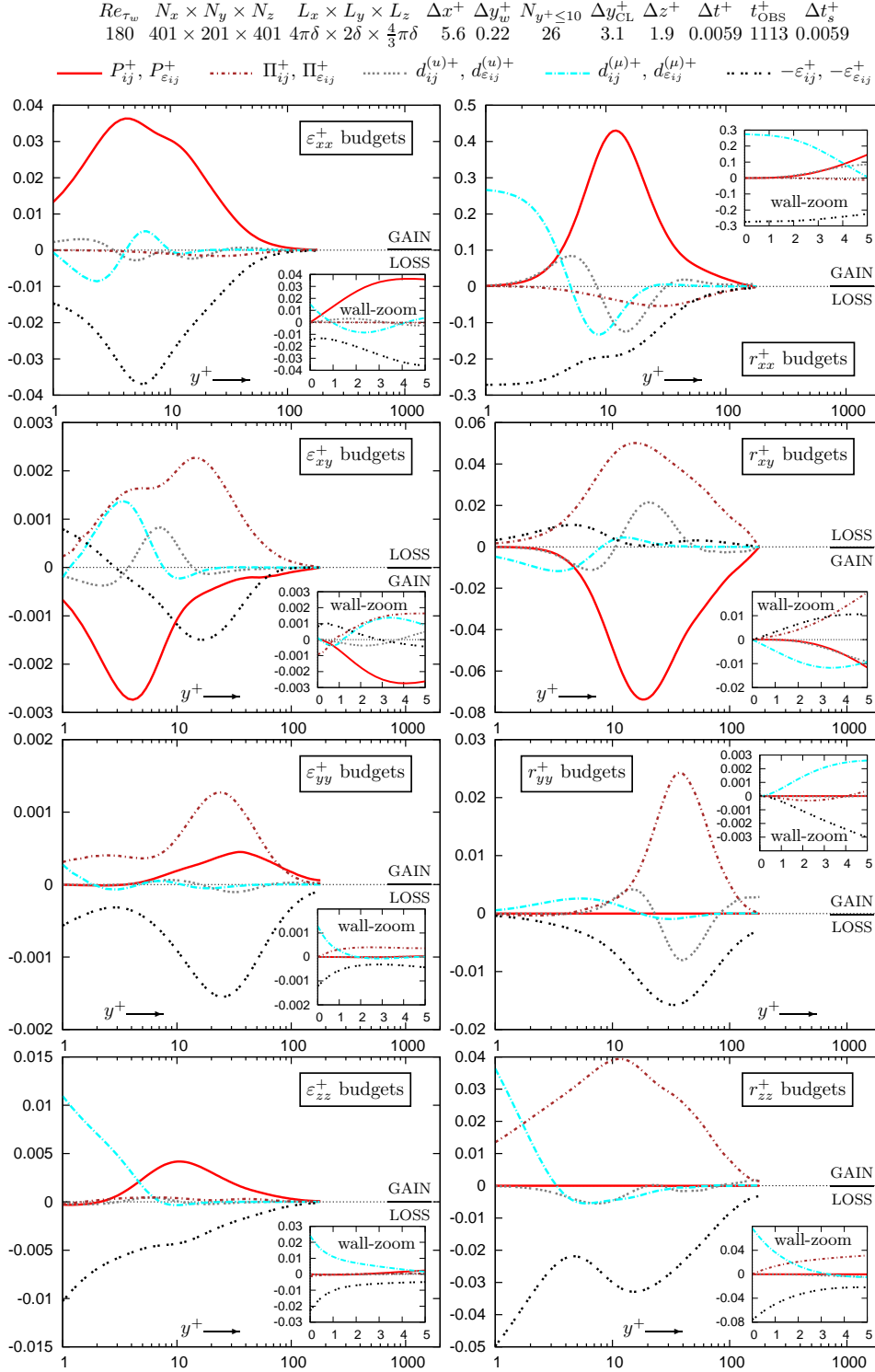


Figure 1. Budgets, in wall-units (Gerolymos and Vallet, 2016a, (A3), p. 414), of the transport equations for the dissipation tensor ε_{ij} (1b) and for the Reynolds-stresses r_{ij} (1a), from the present DNS computations of turbulent plane channel flow ($Re_{\tau_w} \approx 180$), plotted against the inner-scaled wall-distance y^+ (logscale and linear wall-zoom).

by comparison with available (Moser et al., 1999; Hoyas and Jiménez, 2008; Vreman and Kuerten, 2014a; Vreman and Kuerten, 2014b; Vreman and Kuerten, 2016; Lee and Moser, 2015) 1-point and 2-point DNS data (Gerolymos, S  n  chal and Vallet, 2010; Gerolymos, S  n  chal and Vallet, 2013; Gerolymos and Vallet, 2014; Gerolymos and Vallet, 2016a).

The terms in ε_{ij} -transport (1b) contain correlations of 1-order-higher derivatives of fluctuating quantities compared to the corresponding terms in r_{ij} -transport (1a). Therefore, terms in the ε_{ij} -transport equations (1b) are more sensitive to computational truncation errors (Gerolymos, 2011), requiring finer grids to achieve the same accuracy as the corresponding terms in the r_{ij} -transport equations (1a). Furthermore, scaling analysis (Tennekes and Lumley, 1972, pp. 88–92) substantiates that terms in ε_{ij} -transport (1b) are generally related with Taylor-microscale and/or Kolmogorov-scale structures, again suggesting that finer grids are required to obtain these terms than ε_{ij} itself. Accordingly, the computational grid resolution (Figs. 1, 4) was high both streamwise ($\Delta x^+ \approx 5.6$) and spanwise ($\Delta z^+ \approx 1.9$) to correctly predict the details of the elongated near-wall structures (Gerolymos, S  n  chal and Vallet, 2010, Figs. 12–15, pp. 802–805). Finally, several of the terms in ε_{ij} -transport (1b) present important variations in the viscous sublayer ($0 < y^+ \lesssim 3$; Fig. 1), requiring a fine wall-normal grid, not only at the wall ($\Delta y_w^+ \approx 0.22$ was found sufficient), but with weak cell-size stretching to ensure good resolution in the entire near-wall region ($N_{y^+ \leq 10} = 26$ points in the region $0 \leq y^+ < 10$) and actually throughout the entire channel up to the centerline ($\Delta y_{CL}^+ \approx 3.1$). The streamwise resolution is similar to the finest grid used in Vreman and Kuerten (2016) while the present spanwise resolution is roughly twice finer. On the other hand, the present wall-normal resolution is roughly twice coarser compared to Vreman and Kuerten (2016). Although Vreman and Kuerten (2016) did not study the dissipation tensor, their data include the terms in the transport-equations for the variances of the fluctuating velocity-gradients (Vreman and Kuerten, 2014b), which can be combined (Gerolymos and Vallet, 2016a) to obtain the transport equations for the diagonal terms $\{\varepsilon_{xx}, \varepsilon_{yy}, \varepsilon_{zz}\}$ (but not for the shear term ε_{xy}). The 2 sets of data are in very good agreement (Gerolymos and Vallet, 2016a, Figs. 8, 9, pp. 410, 411).

Correlations in (1b) were computed using order-4 inhomogeneous-grid interpolating polynomials (Gerolymos, 2012) and sampled at every iteration ($\Delta t_s^+ = \Delta t^+ \approx 0.0059$) for an observation interval $t_{OBS}^+ \approx 1113$. Because of the relatively short observation interval, the pressure term $\Pi_{\varepsilon_{ij}}$ (1b) which contains the highly intermittent pressure-Hessian (Vreman and Kuerten, 2014b, Fig. 12, p. 21), was calculated from the identity $\Pi_{\varepsilon_{ij}} = d_{\varepsilon_{ij}}^{(p)} + \phi_{\varepsilon_{ij}}$ (4). The RHS terms in (4) only involve fluctuating pressure-gradients and converge much faster.

3.2. ε_{ij} vs r_{ij} budgets

Comparison (Fig. 1) of the budgets of the Reynolds-stresses r_{ij} (1a) with those of the dissipation tensor ε_{ij} (1b), for plane channel flow (§A.2), reveals fundamental differences, both in the relative importance of various mechanisms in the budgets of each component and in the componentality of corresponding mechanisms.

Regarding the importance of different mechanisms in the budgets, it is noticeable that the pressure term $\Pi_{\varepsilon_{ij}}^+$ is negligibly small both for the streamwise ε_{xx}^+ and the spanwise ε_{zz}^+ components (Fig. 1). This difference is especially important in the budgets of the spanwise components, r_{zz}^+ and ε_{zz}^+ . For the spanwise stress r_{zz}^+ , in

plane channel flow (A.1–A.3) there is no production mechanism ($P_{zz}^+ = 0 \forall y^+$) and gain comes mainly from the redistributive action of Π_{ij}^+ (Fig. 1). On the contrary, for the spanwise dissipation ε_{zz}^+ , gain comes mainly from the production terms $P_{\varepsilon_{zz}}^{(2)+} + P_{\varepsilon_{zz}}^{(4)+}$ (A.5d), the pressure term $\Pi_{\varepsilon_{zz}}^+$ being very weak (Fig. 1). Comparison

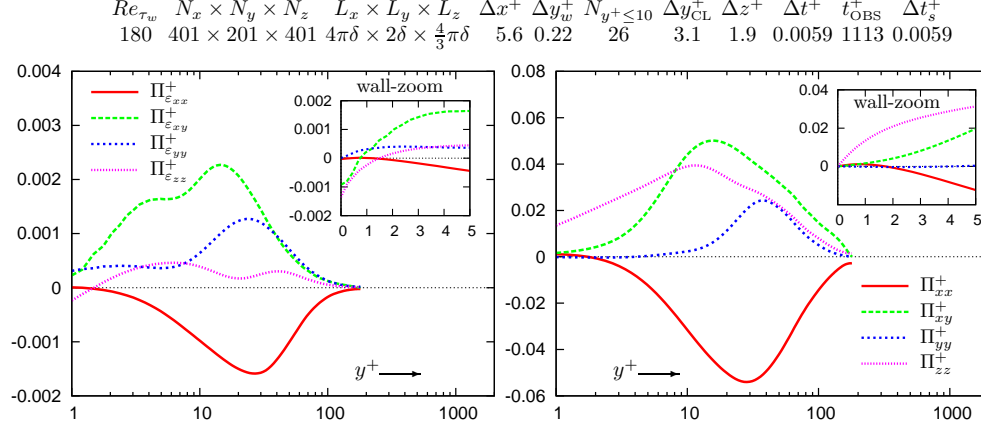


Figure 2. Components, in wall-units (Gerolymos and Vallet, 2016a, (A3), p. 414), of the pressure terms $\Pi_{\varepsilon_{ij}}$ and Π_{ij} in the transport equations for the dissipation tensor ε_{ij} (1b) and for the Reynolds-stresses r_{ij} (1a), from the present DNS computations of turbulent plane channel flow ($Re_{\tau_w} \approx 180$), plotted against the inner-scaled wall-distance y^+ (logscale and linear wall-zoom).

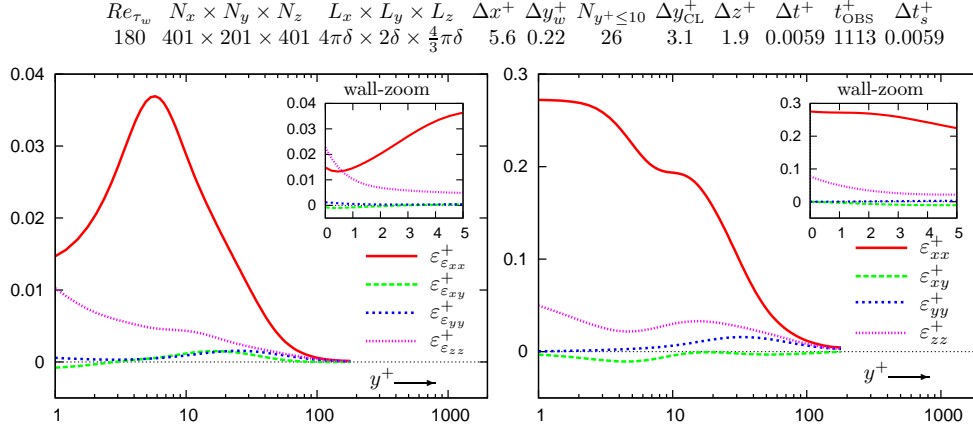


Figure 3. Components, in wall-units (Gerolymos and Vallet, 2016a, (A3), p. 414), of the terms representing destruction by molecular viscosity $\varepsilon_{\varepsilon_{ij}}$ and ε_{ij} in the transport equations for the dissipation tensor ε_{ij} (1b) and for the Reynolds-stresses r_{ij} (1a), from the present DNS computations of turbulent plane channel flow ($Re_{\tau_w} \approx 180$), plotted against the inner-scaled wall-distance y^+ (logscale and linear wall-zoom).

of the componentality of $\Pi_{\varepsilon_{ij}}^+$ with that of Π_{ij}^+ (Fig. 2) reveals that, although all the components of each tensor are of the same order-of-magnitude, $\Pi_{\varepsilon_{zz}}^+$ is consistently weaker than the other components of $\Pi_{\varepsilon_{ij}}^+$ contrary to Π_{zz}^+ which is the largest component of Π_{ij}^+ near the wall ($y^+ \lesssim 10$; Fig. 2). Another important difference

is observed in the limiting behaviour of $\Pi_{\varepsilon_{xy}}^+$ and $\Pi_{\varepsilon_{zz}}^+$ both of which are $\neq 0$ at the wall (Tab. 1) whereas $[\Pi_{ij}]_w^+ = 0$ because of the no-slip condition (A.1a).

The y^+ -distribution (Fig. 3) of the destruction-of-dissipation tensor $\varepsilon_{\varepsilon_{ij}}^+$ (1b) differs substantially from that of the dissipation tensor ε_{ij}^+ (1a). Away from the wall, the streamwise components ε_{xx}^+ and $\varepsilon_{\varepsilon_{xx}}^+$ are in both cases much larger than the other components. Near the wall ε_{xx}^+ forms a small plateau ($y^+ \in [8, 12]$; Fig. 3) and then increases as $y^+ \rightarrow 0$, reaching its global maximum at the wall, remaining by far the largest component of $\varepsilon_{ij}^+ \forall y^+$ (Fig. 3). On the contrary, $\varepsilon_{\varepsilon_{xx}}^+$ reaches its global maximum at $y^+ \approx 7$ and then decreases as $y^+ \rightarrow 0$. At the same time $\varepsilon_{\varepsilon_{zz}}^+$ sharply increases near the wall, the 2 components crossing each other at $y^+ \approx 0.7$ (Fig. 3) to reach $[\varepsilon_{\varepsilon_{zz}}^+]_w^+ > [\varepsilon_{\varepsilon_{xx}}^+]_w^+$. The wall-asymptotic expansion of $\varepsilon_{\varepsilon_{ij}}^+$, as $y^+ \rightarrow 0$, shows (Tab. 2) that all of the $\varepsilon_{\varepsilon_{ij}}^+$ -components are $\neq 0$ at the wall in contrast to ε_{ij}^+ , for which $[\varepsilon_{yy}]_w^+ = [\varepsilon_{xy}]_w^+ = 0$ (Mansour et al., 1988, (16,21), pp. 21–22). Another difference in the componentality of the 2 tensors (Fig. 3) is that while $\varepsilon_{xy}^+ < 0 \forall y^+ \in]0, \delta^+[$, $\varepsilon_{\varepsilon_{xy}}^+ \leq 0 \forall y^+ \lesssim 3$ changes sign further away from the wall ($\varepsilon_{\varepsilon_{xy}}^+ \geq 0 \forall y^+ \gtrsim 3$; Fig. 3). Therefore, while $-\varepsilon_{xy}^+ > 0 \forall y^+ \in]0, \delta^+[$ is a loss mechanism in the budgets of $r_{xy}^+ < 0 \forall y^+ \in]0, \delta^+[$ (Fig. 1), this is not the case for $-\varepsilon_{\varepsilon_{xy}}^+$ which is, in the major part of the channel ($y^+ \gtrsim 3$; Fig. 1), a gain mechanism in the ε_{xy} -budgets. The componentality differences between r_{ij} , its dissipation ε_{ij} and the destruction-of-dissipation $\varepsilon_{\varepsilon_{ij}}$ are further studied in §4.

The most striking componentality difference concerns the production mechanisms, P_{ij}^+ (1a) and $P_{\varepsilon_{ij}}^+$ (1b). In plane channel flow, all of the components of $P_{\varepsilon_{ij}}^+$ are generally $\neq 0$ and contribute as gain to the corresponding ε_{ij}^+ component (Fig. 1), contrary to P_{ij} (in plane channel flow $P_{yy} = P_{zz} = 0 \forall y^+$ Mansour et al., 1988). The production mechanisms (1b) $P_{\varepsilon_{ij}}^{(1)+}$ (by the direct action of the components of ε_{ij}^+ on the mean velocity-gradient) and $P_{\varepsilon_{ij}}^{(3)+}$ (related to the mean velocity-Hessian) have a similar componentality ($P_{\varepsilon_{yy}}^{(1)+} = P_{\varepsilon_{zz}}^{(1)+} = P_{\varepsilon_{yy}}^{(3)+} = P_{\varepsilon_{zz}}^{(3)+} = 0 \forall y^+$) in plane channel flow (A.1–A.3), but this is not the case for the second production by mean velocity-gradient mechanism $P_{\varepsilon_{ij}}^{(2)+}$ nor for the production by the triple correlations of fluctuating velocity-gradients $P_{\varepsilon_{ij}}^{(4)+}$, both of which are generally $\neq 0$ for all of the components (Gerolymos and Vallet, 2016a, Fig. 6, p. 407).

At the wall ($y^+ = 0$), production $P_{\varepsilon_{ij}}^+$ and turbulent diffusion by the fluctuating velocities $d_{\varepsilon_{ij}}^{(u)+}$ are 0

$$(\text{Tabs. 1, 2}) \implies [P_{\varepsilon_{ij}}]_w^+ = [d_{\varepsilon_{ij}}^{(u)}]_w^+ = 0 \quad (3a)$$

so that the wall-budgets of the ε_{ij} -transport equations (A.4, A.5) reduce to

$$(\text{Tabs. 1, 2}) \implies [d_{\varepsilon_{ij}}^{(\mu)}]_w^+ + [\Pi_{\varepsilon_{ij}}]_w^+ = [\varepsilon_{\varepsilon_{ij}}]_w^+ \quad (3b)$$

In the particular case of the wall-normal diagonal component $[\Pi_{\varepsilon_{yy}}]_w^+ = 0$ (Tab. 1), implying $[d_{\varepsilon_{yy}}^{(\mu)}]_w^+ = [\varepsilon_{\varepsilon_{yy}}]_w^+ = \overline{16B_v'^+{}^2}$ (Tabs. 1, 2). Notice also that, by (B.5), the halftrace $\frac{1}{2}[\Pi_{\varepsilon_{\ell\ell}}]_w^+ \stackrel{(\text{Tab. 1})}{=} -8B_v'^+{}^2$ in agreement with Mansour et al. (1988, (24), p. 24).

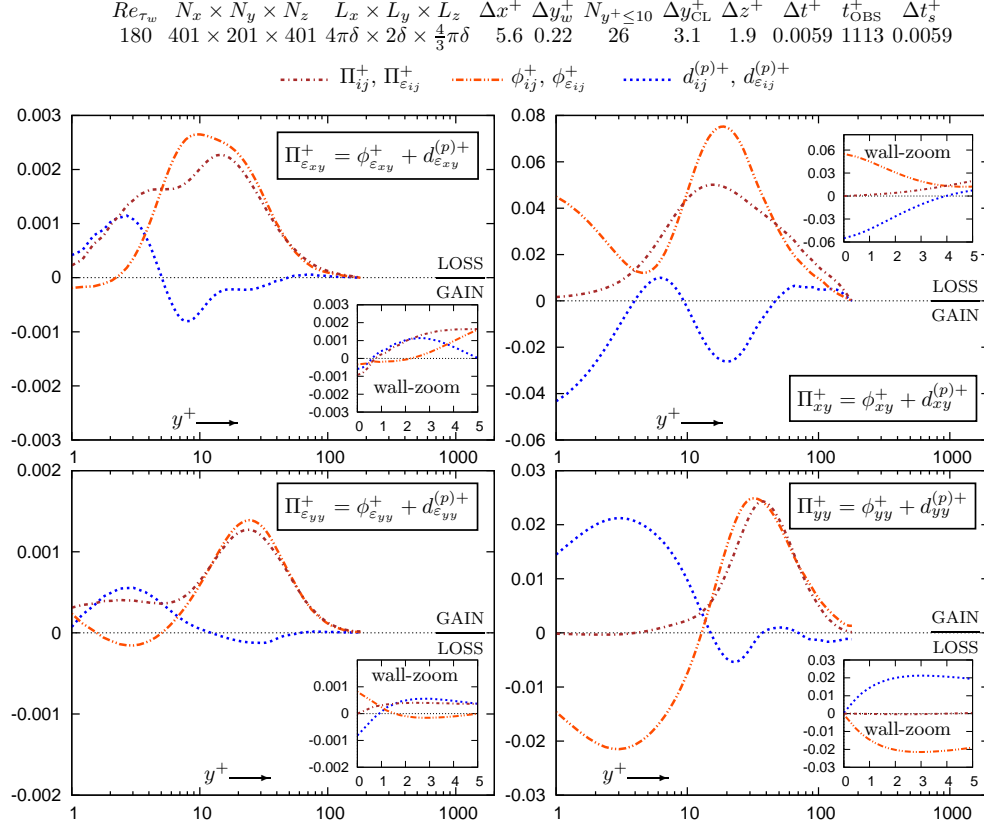


Figure 4. Splitting (4, 5), of wall-normal and shear components (in plane channel flow $d_{\varepsilon_{xx}}^{(p)+} = d_{\varepsilon_{zz}}^{(p)+} = d_{xx}^{(p)+} = d_{zz}^{(p)+} = 0 \forall y^+$) of the pressure terms $\Pi_{\varepsilon_{ij}}$ and Π_{ij} in the transport equations for the dissipation tensor ε_{ij} (1b) and for the Reynolds-stresses r_{ij} (1a), into redistribution ($\Pi_{\varepsilon_{ij}}$ and Π_{ij}) and pressure diffusion ($d_{\varepsilon_{ij}}^{(p)}$ and $d_{ij}^{(p)}$), in wall-units (Gerolymos and Vallet, 2016a, (A3), p. 414), from the present DNS computations of turbulent plane channel flow ($Re_{\tau_w} \approx 180$), plotted against the inner-scaled wall-distance y^+ (logscale and linear wall-zoom).

3.3. Redistribution and pressure-diffusion

In exact analogy with r_{ij} -transport (1a), where by application of the product-rule of differentiation (Riley et al., 2006, §2.12, pp. 44-46), the velocity/pressure-gradient correlation Π_{ij} (1a) can be split into pressure diffusion $d_{ij}^{(p)}$ and a redistributive term ϕ_{ij}

$$\Pi_{ij} \stackrel{(1a)}{=} \underbrace{\frac{\partial}{\partial x_\ell} \left(-\delta_{i\ell} \overline{u'_j p'} - \delta_{j\ell} \overline{u'_i p'} \right)}_{d_{ij}^{(p)}} + \underbrace{p' \left(\frac{\partial u'_i}{\partial x_j} + \frac{\partial u'_j}{\partial x_i} \right)}_{\phi_{ij}} \quad (4a)$$

with

$$\phi_{mm} \stackrel{(4a, B.3)}{=} 0 \stackrel{(4a)}{\implies} \Pi_{mm} = d_{mm}^{(p)} \stackrel{(4a)}{=} \frac{\partial}{\partial x_\ell} \left(-2\overline{u'_\ell p'} \right) \quad (4b)$$

the pressure term $\Pi_{\varepsilon_{ij}}$ in (1b) can be split into pressure diffusion $d_{\varepsilon_{ij}}^{(p)}$ and a redistributive term $\phi_{\varepsilon_{ij}}$, viz

$$\Pi_{\varepsilon_{ij}} \stackrel{(1b)}{=} \underbrace{\frac{\partial}{\partial x_\ell} \left(-2\nu\delta_{i\ell} \frac{\partial u'_j}{\partial x_k} \frac{\partial p'}{\partial x_k} - 2\nu\delta_{j\ell} \frac{\partial u'_i}{\partial x_k} \frac{\partial p'}{\partial x_k} \right)}_{d_{\varepsilon_{ij}}^{(p)}} + \underbrace{2\nu \frac{\partial p'}{\partial x_k} \left[\frac{\partial}{\partial x_k} \left(\frac{\partial u'_i}{\partial x_j} + \frac{\partial u'_j}{\partial x_i} \right) \right]}_{\phi_{\varepsilon_{ij}}} \quad (5a)$$

with

$$\phi_{\varepsilon_{mm}} \stackrel{(5a, B.3)}{=} 0 \stackrel{(5a)}{\implies} \Pi_{\varepsilon_{mm}} = d_{\varepsilon_{mm}}^{(p)} \stackrel{(5a)}{=} \frac{\partial}{\partial x_\ell} \left(-4\nu \frac{\partial u'_\ell}{\partial x_k} \frac{\partial p'}{\partial x_k} \right) \quad (5b)$$

Because of the incompressible fluctuating continuity (B.3), $\phi_{\varepsilon_{ij}}$ (5a) is traceless (5b), exactly like ϕ_{ij} (4). Therefore it does not appear in the transport equation for the dissipation-rate ε of the turbulence kinetic energy (Mansour et al., 1988, (23), p. 23) and has a redistribution role among components of ε_{ij} . In second-moment closures, ϕ_{ij} (4) occupies a central place (Launder et al., 1975; Speziale, Sarkar and Gatski, 1991; Gerolymos, Lo and Vallet, 2012; Jakirlić and Hanjalić, 2013) in modelling work, because pressure diffusion $d_{ij}^{(p)}$ is absent in homogeneous flows. It is therefore interesting to investigate (Fig. 4) the splitting (5) of $\Pi_{\varepsilon_{ij}}$ in comparison with the splitting of Π_{ij} (4). Since only y -gradients of second-moments of fluctuating quantities are $\neq 0$ in plane channel flow (A.3) the splittings (4, 5) are only relevant for the wall-normal and the shear components (in plane channel flow $d_{\varepsilon_{xx}}^{(p)+} = d_{\varepsilon_{zz}}^{(p)+} = d_{xx}^{(p)+} = d_{zz}^{(p)+} = 0 \forall y^+$).

As already observed in the analysis of r_{ij} -transport (Mansour et al., 1988), pressure diffusion is generally weak away from the wall, so that (Fig. 4) both $\Pi_{\varepsilon_{yy}} \approx \phi_{\varepsilon_{yy}} \forall y^+ \gtrsim 10$ and $\Pi_{yy} \approx \phi_{yy} \forall y^+ \gtrsim 10$. These approximate equalities also apply for the shear components, but for higher $y^+ \gtrsim 30$ (Fig. 4). This implies that modelling $\phi_{\varepsilon_{ij}}$ in lieu of $\Pi_{\varepsilon_{ij}}$ in the log-region of the velocity profile (Coles, 1956) could be a reasonable working choice, exactly like in r_{ij} -transport models (Launder et al., 1975). On the other hand, nearer to the wall ($1 \lesssim y^+ \lesssim 10$; Fig. 4) the splittings of $\Pi_{\varepsilon_{ij}}$ (5) and Π_{ij} (4) are quite different. Regarding Π_{ij} , both Π_{yy} and Π_{xy} are very small for $y^+ \lesssim 5$, so that $\phi_{yy} \approx -d_{yy}^{(p)} \forall y^+ \lesssim 8$ and $\phi_{xy} \approx -d_{xy}^{(p)} \forall y^+ \lesssim 4$ (Fig. 4), but this does not apply to $\Pi_{\varepsilon_{ij}}$. Notice also that while $[\Pi_{ij}]_w \stackrel{(1a, B.3)}{=} 0$ because of the no-slip condition at the wall this is not the case for $\Pi_{\varepsilon_{ij}}$ (only the wall-normal component $[\Pi_{\varepsilon_{yy}}]_w = 0$ at the wall; Tab. 1). These differences in near-wall behaviour between $\Pi_{\varepsilon_{ij}}$ and Π_{ij} should be kept in mind in modelling efforts of the pressure terms in differential ε_{ij} -transport closures.

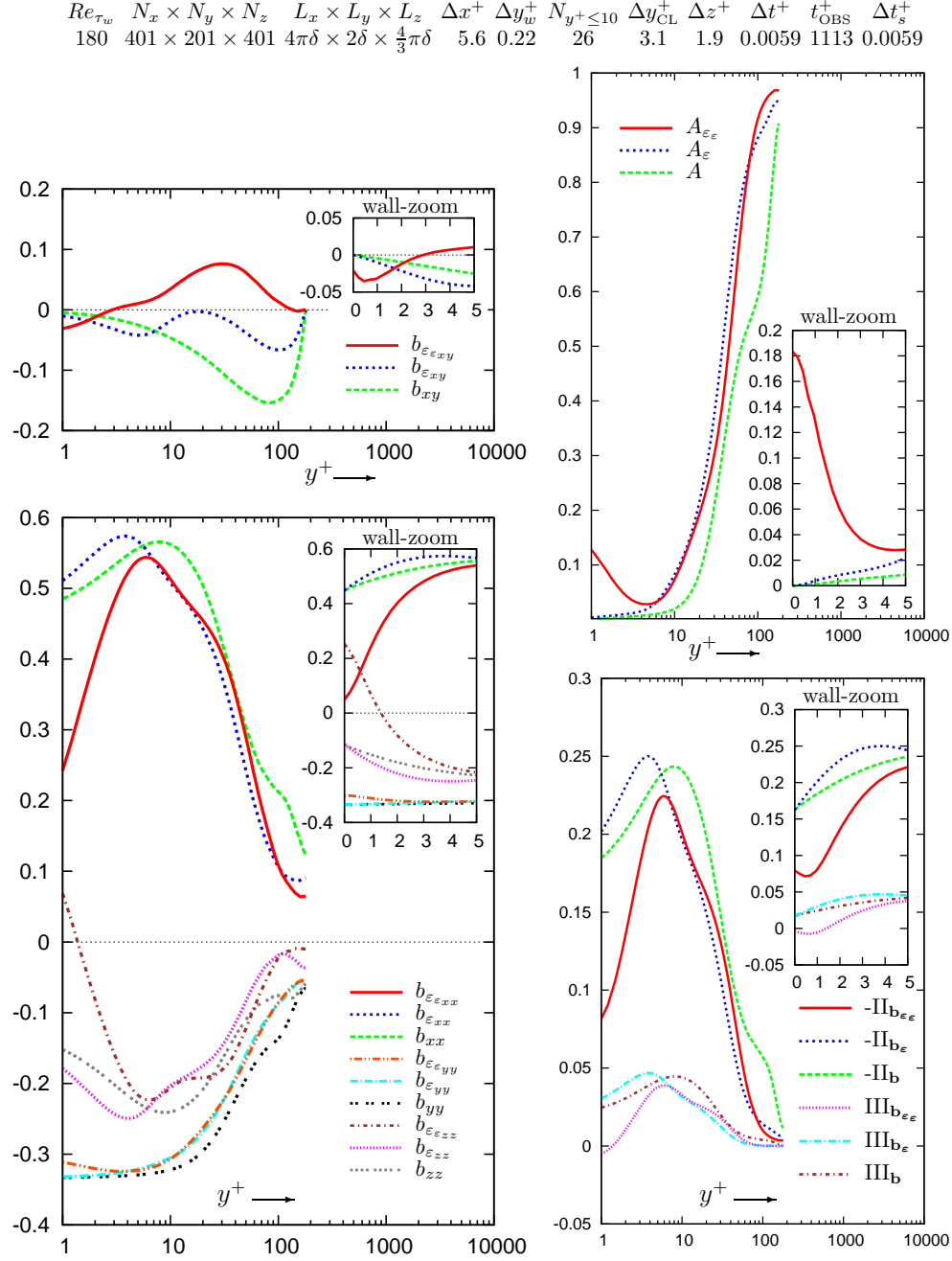


Figure 5. Components and invariants of the anisotropy tensors of the Reynolds-stresses b_{ij} (7a), of the dissipation tensor $b_{\varepsilon_{ij}}$ (7b) and of the destruction-of-dissipation tensor $b_{\varepsilon_{\varepsilon_{ij}}}$ (7c), from the present DNS computations of turbulent plane channel flow ($Re_{\tau_w} \approx 180$), plotted against the inner-scaled wall-distance y^+ (logscale and linear wall-zoom).

$$\begin{aligned}
\varepsilon_{\varepsilon_{xx}}^+ &\sim 8 \left(2 \overline{B_u'^+}^2 + \overline{(\nabla A_u')^+}^2 \right) + 32 \left(3 \overline{B_u'^+ C_u'^+} + \overline{(\nabla A_u')^+ \cdot (\nabla B_u')^+} \right) y^+ + O(y^{+2}) \\
\varepsilon_{\varepsilon_{xy}}^+ &\sim 16 \overline{B_u'^+ B_v'^+} + 16 \left(3 \overline{B_v'^+ C_u'^+} + \left\{ 3 \overline{B_u'^+ C_v'^+} \right\} + \overline{(\nabla A_u')^+ \cdot (\nabla B_v')^+} \right) y^+ + O(y^{+2}) \\
\varepsilon_{\varepsilon_{yy}}^+ &\sim 16 \overline{B_v'^+}^2 + 96 \overline{B_v'^+ C_v'^+} y^+ + O(y^{+2}) \\
\varepsilon_{\varepsilon_{yz}}^+ &\sim \left[16 \overline{B_w'^+ B_v'^+} + 16 \left(3 \overline{B_v'^+ C_w'^+} + 3 \overline{B_w'^+ C_v'^+} + \overline{(\nabla A_w')^+ \cdot (\nabla B_v')^+} \right) y^+ + O(y^{+2}) \right] \\
\varepsilon_{\varepsilon_{zz}}^+ &\sim 8 \left(2 \overline{B_w'^+}^2 + \overline{(\nabla A_w')^+}^2 \right) + 32 \left(3 \overline{B_w'^+ C_w'^+} + \overline{(\nabla A_w')^+ \cdot (\nabla B_w')^+} \right) y^+ + O(y^{+2}) \\
\varepsilon_{\varepsilon_{zx}}^+ &\sim \left[8 \left(2 \overline{B_u'^+ B_w'^+} + \overline{(\nabla A_u')^+ \cdot (\nabla A_w')^+} \right) \right. \\
&\quad \left. + 16 \left(3 \overline{B_u'^+ C_w'^+} + 3 \overline{B_w'^+ C_u'^+} + \overline{(\nabla A_u')^+ \cdot (\nabla B_w')^+} + \overline{(\nabla A_w')^+ \cdot (\nabla B_u')^+} \right) y^+ + O(y^{+2}) \right]
\end{aligned}$$

Table 3. Asymptotic (as $y^+ \rightarrow 0$) expansions of the components of $\varepsilon_{\varepsilon}$ (1b), in wall-units (Gerolymos and Vallet, 2016a, (A3), p. 414), for general inhomogeneous incompressible turbulent flow near a plane no-slip xz -wall (terms within square brackets $[\dots]$ are 3-D terms which are identically = 0 for 2-D in-the-mean flow whereas the term within curly brackets $\{\dots\}$ in ε_{xy}^+ , $B_u'^+ C_v'^+ = 0$ (B.11c) in the particular case of plane channel flow).

4. Destruction-of-dissipation tensor $\varepsilon_{\varepsilon_{ij}}$

The diagonal components and traces of the 3 tensors

$$r_{ij} := \overline{u'_i u'_j} \implies r_{xx}, r_{yy}, r_{zz} \geq 0 \leq k := \frac{1}{2} \overline{u'_m u'_m} \quad (6a)$$

$$\varepsilon_{ij} := 2\nu \overline{\frac{\partial u'_i}{\partial x_\ell} \frac{\partial u'_j}{\partial x_\ell}} \implies \varepsilon_{xx}, \varepsilon_{yy}, \varepsilon_{zz} \geq 0 \leq \varepsilon := \frac{1}{2} \varepsilon_{mm} \quad (6b)$$

$$\varepsilon_{\varepsilon_{ij}} := 4\nu^2 \overline{\frac{\partial^2 u'_i}{\partial x_k \partial x_\ell} \frac{\partial^2 u'_j}{\partial x_k \partial x_\ell}} \implies \varepsilon_{\varepsilon_{xx}}, \varepsilon_{\varepsilon_{yy}}, \varepsilon_{\varepsilon_{zz}} \geq 0 \leq \varepsilon_{\varepsilon} := \frac{1}{2} \varepsilon_{\varepsilon_{mm}} \quad (6c)$$

are positive in every frame-of-reference. Therefore these tensors are positive-definite (Gerolymos and Vallet, 2016a) implying that the invariants (Rivlin, 1955) of the corresponding traceless anisotropy tensors (Gerolymos, Lo and Vallet, 2012)

$$b_{ij} := \frac{\overline{u'_i u'_j}}{2k} - \frac{1}{3} \delta_{ij} \quad ; \quad \Pi_{\mathbf{b}} = -\frac{1}{2} b_{mk} b_{km} \quad ; \quad \text{III}_{\mathbf{b}} = \frac{1}{3} b_{mk} b_{kl} b_{lm} \quad (7a)$$

$$b_{\varepsilon_{ij}} := \frac{\varepsilon_{ij}}{2\varepsilon} - \frac{1}{3} \delta_{ij} \quad ; \quad \Pi_{\mathbf{b}_{\varepsilon}} = -\frac{1}{2} b_{\varepsilon_{mk}} b_{\varepsilon_{km}} \quad ; \quad \text{III}_{\mathbf{b}_{\varepsilon}} = \frac{1}{3} b_{\varepsilon_{mk}} b_{\varepsilon_{kl}} b_{\varepsilon_{lm}} \quad (7b)$$

$$b_{\varepsilon_{\varepsilon_{ij}}} := \frac{\varepsilon_{\varepsilon_{ij}}}{2\varepsilon_{\varepsilon}} - \frac{1}{3} \delta_{ij} \quad ; \quad \Pi_{\mathbf{b}_{\varepsilon_{\varepsilon}}} = -\frac{1}{2} b_{\varepsilon_{\varepsilon_{mk}}} b_{\varepsilon_{\varepsilon_{km}}} \quad ; \quad \text{III}_{\mathbf{b}_{\varepsilon_{\varepsilon}}} = \frac{1}{3} b_{\varepsilon_{\varepsilon_{mk}}} b_{\varepsilon_{\varepsilon_{kl}}} b_{\varepsilon_{\varepsilon_{lm}}} \quad (7c)$$

[illegible]

Table 4. Asymptotic (as $y^+ \rightarrow 0$) expansions of the components of $\mathbf{b}_{\epsilon\epsilon}$ (6c), in wall-units (Gerolymos and Vallet, 2016a, (A3), p. 414), for general inhomogeneous incompressible turbulent flow near a plane no-slip xz -wall (terms within square brackets $\{\dots\}$ are 3-D terms which are identically = 0 for 2-D in-the-mean flow whereas the term within curly brackets $\{\dots\}$ in $b_{\epsilon xy}$, $B_u^{++}C_v^{++} = 0$ (B.11c) in the particular case of plane channel flow).

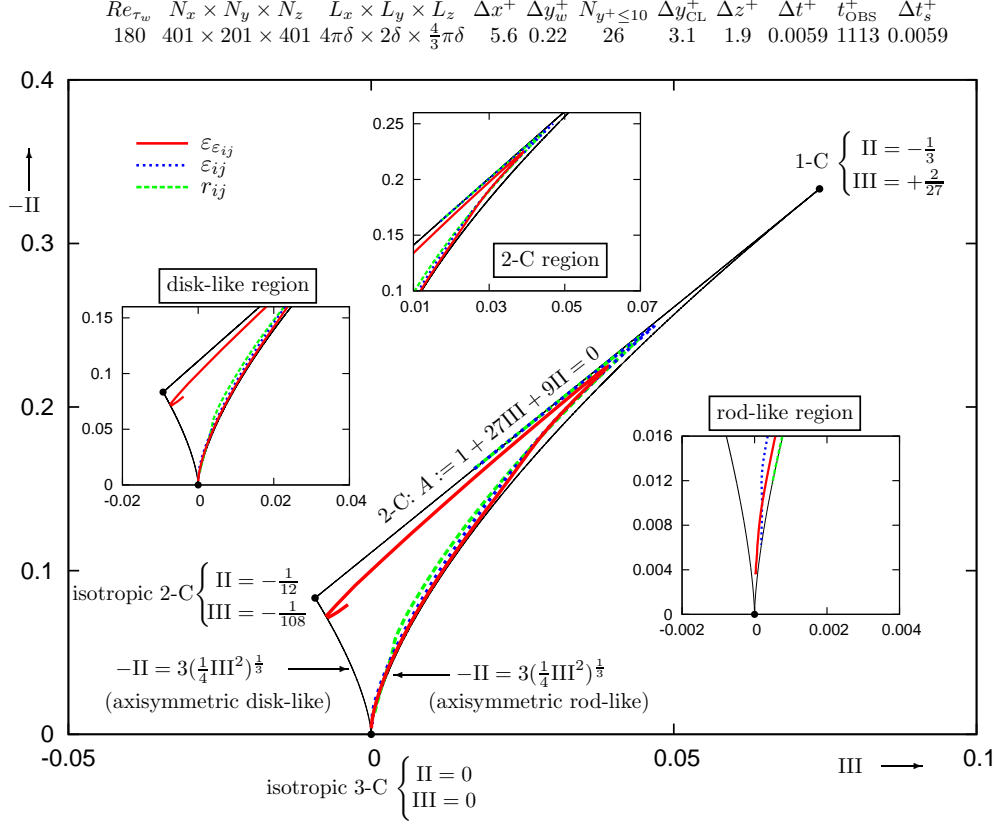


Figure 6. Lumley's (1978) realizability triangle (Simonsen and Krogstad, 2005) in the $(-II, III)$ -plane (7) and trajectory in the wall-normal direction of the locus of the anisotropy-tensor invariants of the Reynolds-stresses b_{ij} (7a), of the dissipation tensor $b_{\varepsilon_{ij}}$ (7b) and of the destruction-of-dissipation tensor $b_{\varepsilon_{\varepsilon_{ij}}}$ (7c), from the present DNS computations of turbulent plane channel flow ($Re_{\tau_w} \approx 180$).

lie within Lumley's (1978) realisability triangle in the $(III, -II)$ -plane (Gerolymos and Vallet, 2016a). Lumley's (1978) flatness parameters

$$A := 1 + 27III_b + 9II_b \quad ; \quad A_\varepsilon := 1 + 27III_{b_\varepsilon} + 9II_{b_\varepsilon} \quad ; \quad A_{\varepsilon_\varepsilon} := 1 + 27III_{b_{\varepsilon_\varepsilon}} + 9II_{b_{\varepsilon_\varepsilon}} \quad (7d)$$

are bounded in the interval $[0, 1]$ (Lumley, 1978), between the 2-component (2-C) limit corresponding to the value 0 and the isotropic componentality corresponding to the value 1 (Simonsen and Krogstad, 2005). It is well known (Mansour et al., 1988) that at the wall both \mathbf{r} and $\boldsymbol{\varepsilon}$ reach the 2-C limit at the wall. It was recently shown (Gerolymos and Vallet, 2016a) that the 2-C limit at the wall is approached quadratically ($A_\varepsilon \sim_{y^+ \rightarrow 0} 4A \sim_{y^+ \rightarrow 0} O(y^{+2})$). This result was obtained by calculating the wall-asymptotic expansions of \mathbf{b} (Gerolymos and Vallet, 2016a, Tab. 1, p. 392) and of \mathbf{b}_ε (Gerolymos and Vallet, 2016a, Tab. 2, p. 393) and of their invariants. However, as shown previously (Fig. 3) $\boldsymbol{\varepsilon}_\varepsilon$ is not 2-C at the wall, where all of its components are generally $\neq 0$ (Tabs. 2, 3).

These differences in behaviour are better understood by considering (Fig. 5)

the anisotropy tensors $\{\mathbf{b}, \mathbf{b}_\varepsilon, \mathbf{b}_{\varepsilon_\varepsilon}\}$ and their invariants (7). Although the shear components $\{r_{xy}^+, \varepsilon_{xy}^+, \varepsilon_{\varepsilon xy}^+\}$ are invariably much smaller than the traces $\{k^+, \varepsilon^+, \varepsilon_\varepsilon^+\}$ (6), their anisotropy (Fig. 5) highlights some fundamental differences between the 3 tensors. The shear Reynolds-stress is $r_{xy}^+ < 0 \forall y^+ \in]0, \delta^+[$ (sign $r_{xy} = \text{sign } b_{xy}$; Fig. 5), whereas $\varepsilon_{xy}^+ < 0 \forall y^+ \in]0, \delta^+[$ is close to 0 at $y^+ \approx 25$ (Fig. 5), $\varepsilon_{\varepsilon xy}^+$ exhibiting a radically different behaviour (Figs. 3, 5). The wall-asymptotic expansion of $\mathbf{b}_{\varepsilon_\varepsilon}$ (Tab. 4) confirms that ε_ε is not 2-C at the wall, contrary to \mathbf{b} (Gerolymos and Vallet, 2016a, Tab. 1, p. 392) and \mathbf{b}_ε (Gerolymos and Vallet, 2016a, Tab. 2, p. 393). This is clearly shown by the y^+ -distribution of the corresponding flatness parameter (7d) $A_{\varepsilon_\varepsilon} > 0 \forall y^+$ (Fig. 5), which reaches its minimum value ≈ 0.03 at $y^+ \approx 5$, then increasing to $[A_{\varepsilon_\varepsilon}]_w \approx 0.185$. These differences in near-wall behaviour are also particularly visible in the y^+ -distribution of the anisotropy invariants (Fig. 5) and in the anisotropy invariant mapping (AIM) of ε_ε (Fig. 6). The locus of $\{\text{III}_{\mathbf{b}_\varepsilon}, -\text{II}_{\mathbf{b}_\varepsilon}\}$ does not reach the 2-C boundary (Fig. 6). Instead, near the wall, $\{\text{III}_{\mathbf{b}_\varepsilon}, -\text{II}_{\mathbf{b}_\varepsilon}\}$ reaches the axisymmetric disk-like boundary of Lumley's (1978) realisability triangle (Fig. 6), roughly corresponding to $y^+ \approx 0.7$ where $\varepsilon_{xx}^+ = \varepsilon_{zz}^+$ (Fig. 3) and $b_{\varepsilon_{xx}} = b_{\varepsilon_{zz}}$ (Fig. 5), also marked by the near-wall minimum of $\text{III}_{\mathbf{b}_\varepsilon}$ (Fig. 5). For $y^+ \lesssim 0.7$, the locus of $\mathbf{b}_{\varepsilon_\varepsilon}$ in the $(\text{III}_{\mathbf{b}_{\varepsilon_\varepsilon}}, -\text{II}_{\mathbf{b}_{\varepsilon_\varepsilon}})$ -plane returns toward the interior of Lumley's (1978) realisability triangle (Fig. 6). The contrasting behaviour of $\mathbf{b}_{\varepsilon_\varepsilon}$ compared to \mathbf{b} and \mathbf{b}_ε (Figs. 5, 6) further highlights the complexity of near-wall turbulence, where 2-C componentality at the wall applies to both \mathbf{r} and ε but not to ε_ε . Examination of the wall-asymptotic behaviour of various terms in the ε_{ij} -budgets (Tabs. 1, 2) reveals that neither $d_{\varepsilon_{ij}}^{(\mu)}$ nor $\Pi_{\varepsilon_{ij}}$ are 2-C at the wall, in line with (3b), whereas $P_{\varepsilon_{ij}}$ and $d_{\varepsilon_{ij}}^{(u)}$ are 2-C at the wall (Tabs. 1, 2). Notice in particular the wall-behaviour of $\Pi_{\varepsilon_{ij}}$, for which $[\Pi_{\varepsilon_{xy}}]_w^+ \neq 0$ while $[\Pi_{\varepsilon_{yy}}]_w^+ = 0$ (Tab. 1). Notice also that, at the wall, $\varepsilon_{\varepsilon w}^{-1} \varepsilon_w$ defines, by dimensional analysis (Tennekes and Lumley, 1972, p. 5), a time-scale which is finite contrary to $k_w \varepsilon_w^{-1} = 0$.

5. Conclusions

The paper studies ε_{ij} -budgets, including the shear component, and compares the behaviour of different mechanisms with the corresponding mechanisms in r_{ij} -budgets, using novel DNS data for low $Re_{\tau_w} \approx 180$ plane channel flow.

All of the components of production $P_{\varepsilon_{ij}}$ are generally $\neq 0$ (specifically all of the components of $P_{\varepsilon_{ij}}^{(2)}$ and $P_{\varepsilon_{ij}}^{(4)}$) and contribute as gain to the corresponding ε_{ij} -budgets, contrary to the r_{ij} -budgets where for plane channel flow $P_{yy} = P_{zz} = 0 \forall y^+$. The pressure mechanism $\Pi_{\varepsilon_{ij}}$ has a very weak contribution to the budgets of the streamwise ε_{xx} and spanwise ε_{zz} components, in contrast to Π_{ij} which is important in the budgets of all r_{ij} -components, especially in the log-region. The destruction-of-dissipation tensor $\varepsilon_{\varepsilon_{ij}}$ behaves very differently from the dissipation tensor ε_{ij} . The shear component $\varepsilon_{\varepsilon_{xy}} > 0 \forall y^+ \gtrsim 3$ is a gain mechanism in the ε_{xy} -budgets except very near the wall ($y^+ \lesssim 3$), contrary to $\varepsilon_{xy} < 0 \forall y^+ \in]0, \delta^+[$ which is a loss mechanism in the r_{xy} -budgets. Finally, analytical results and DNS data for the wall-asymptotic behaviour of different terms in the ε_{ij} -budgets show that the wall boundary-condition is $[d_{\varepsilon_{ij}}^{(\mu)}]_w^+ + [\Pi_{\varepsilon_{ij}}]_w^+ = [\varepsilon_{\varepsilon_{ij}}]_w^+$ instead of the well known condition $[d_{ij}^{(\mu)}]_w^+ = [\varepsilon_{ij}]_w^+$ for the r_{ij} -budgets (Mansour et al., 1988).

All of the 3 tensors (r_{ij} , ε_{ij} and $\varepsilon_{\varepsilon_{ij}}$) being positive-definite, their anisotropy was studied using AIM (Lee and Reynolds, 1987), revealing in particular that, near the

wall, the destruction-of-dissipation tensor $\varepsilon_{\varepsilon_{ij}}$, after reaching the axisymmetric disk-like boundary (roughly where $\varepsilon_{\varepsilon_{xx}} \approx \varepsilon_{\varepsilon_{zz}}$, at $y^+ \approx 0.7$), returns inside the realisability triangle, never approaching the 2-C boundary. The DNS data are corroborated by the wall-asymptotic expansions of $\varepsilon_{\varepsilon_{ij}}$ and of its anisotropy tensor $b_{\varepsilon_{ij}}$. This observed componentality of $\varepsilon_{\varepsilon_{ij}}$ is strikingly different from that of r_{ij} or ε_{ij} , both of which are 2-C at the wall, and highlights the difference between componentality of various tensors and dimensionality of turbulence (Kassinos et al., 2001).

The analysis of the DNS data highlights the complexity of ε_{ij} -transport, especially near the wall and regarding the shear component ε_{xy} . It seems plausible that the specific behaviour of the ε_{xy} -budgets, both with respect to r_{xy} -budgets and compared to the diagonal components of ε_{ij} , can only be modelled by differential r_{ij} - ε_{ij} closures. It is hoped that the present DNS data will be useful in the development of such closures.

Acknowledgments

The authors are listed alphabetically. The computations reported in the present work were performed using HPC ressources allocated at GENCI-IDRIS (Grant 2015–022139) and at ICS–UPMC (ANR–10–EQPX–29–01). Tabulated DNS data are available at http://www.aerodynamics.fr/DNS_database/CT_chnnl. The present work was partly supported by the ANR project NumERICCS(ANR–15–CE06–0009).

Appendix A. Fully developed plane channel flow

We consider fully developed (xz -invariant) plane channel flow (the channel height is 2δ and xyz are respectively the streamwise, wall-normal and spanwise directions) and use nondimensional inner variables (Gerolymos and Vallet, 2016a, wall-units, (A.3), p. 414).

A.1. Mean-flow and symmetries

No-slip boundary-conditions apply at the walls

$$y^+ \in \{0, 2\delta^+\} \implies \bar{u}^+ = \bar{v}^+ = \bar{w}^+ = u'^+ = v'^+ = w'^+ = 0 ; \forall x^+, z^+, t^+ \quad (\text{A.1a})$$

The usual hypotheses that the mean-flow is steady, 2-D and that the x -wise location that is investigated is sufficiently downstream of the channel inlet to achieve fully developed flow (Zanoun, Nagig and Durst, 2009; Schultz and Flack, 2013) in the streamwise direction

$$\frac{\partial(\cdot)}{\partial t^+} = 0 ; \bar{w}^+ = 0 ; r_{yz}^+ = r_{zx}^+ = 0 ; \frac{\partial(\cdot)}{\partial z^+} = 0 ; \frac{\partial \bar{u}_i^+}{\partial x^+} = 0 ; \frac{\partial r_{ij}^+}{\partial x^+} = 0 \quad (\text{A.1b})$$

are made. Under these conditions (A.1), the mean continuity (Mathieu and Scott, 2000, (4.5), p. 76) and momentum (streamwise and wall-normal) equations (Mathieu and Scott, 2000, (4.9), p. 77), imply (Mathieu and Scott, 2000, pp. 105–

111) the exact relations

$$\bar{v}^+ = 0 \quad \forall x^+, y^+ \quad (\text{A.2a})$$

$$\frac{\partial \bar{p}^+}{\partial x^+} = \frac{d\bar{p}_w^+}{dx^+} = - \left[\frac{\tau_w}{\delta} \right]^+ = - \frac{1}{\delta^+} = - \frac{1}{Re_{\tau_w}} = \text{const} \quad \forall x^+, y^+ \quad (\text{A.2b})$$

$$-r_{xy}^+ + \frac{d\bar{u}^+}{dy^+} = \left(1 - \frac{y^+}{Re_{\tau_w}} \right) \quad (\text{A.2c})$$

$$\bar{p}^+(x^+, y^+) = \bar{p}_w^+(x^+) - r_{yy}^+(y^+) \quad (\text{A.2d})$$

for the mean streamwise velocity $\bar{u}^+(y^+)$ and mean pressure $\bar{p}^+(x^+, y^+)$ fields, with a constant streamwise pressure-gradient $\partial_x \bar{p} = d_x \bar{p}_w = \text{const}$ (A.2b). In (A.2b, A.2c) $Re_{\tau_w} = \delta^+$ is the friction Reynolds number (Gerolymos and Vallet, 2016a, (A.3g), p. 414). In (A.1, A.2) deterministic potential body-forces (*eg* gravity) in the momentum equations are included in the mean-pressure field (Monin and Yaglom, 1971, p. 31). Recall that the xzt -homogeneity of the averages implies the relations

$$\frac{\partial \overline{(\cdot)'[\cdot]'}}{\partial q} = 0 \implies \overline{(\cdot)' \frac{\partial [\cdot]'}{\partial q}} = - \overline{[\cdot]' \frac{\partial (\cdot)'}{\partial q}} \quad \forall q \in \{x, z, t\} \quad (\text{A.3a})$$

$$\overline{(\cdot)' \frac{\partial^2 [\cdot]'}{\partial q_1 \partial q_2}} = - \frac{\overline{\partial (\cdot)'}}{\partial q_1} \frac{\overline{\partial [\cdot]'}}{\partial q_2} = - \frac{\overline{\partial [\cdot]'}}{\partial q_1} \frac{\overline{\partial (\cdot)'}}{\partial q_2} \quad \forall q_1, q_2 \in \{x, z, t\} \quad (\text{A.3b})$$

A.2. ε_{ij} -budgets in plane channel flow

Under fully developed plane channel flow conditions (A.1, A.2) the ε_{ij} -transport equations simplify to

$$\begin{aligned} (1b, \text{A.1, A.2}) \implies & \underbrace{\frac{d}{dy} \left[-\rho \left(\overline{v' 2\nu \frac{\partial u'_i}{\partial x_k} \frac{\partial u'_j}{\partial x_k}} \right) \right]}_{d_{\varepsilon_{ij}}^{(u)}} + \underbrace{\mu \frac{d^2 \varepsilon_{ij}}{dy^2}}_{d_{\varepsilon_{ij}}^{(\mu)}} - \underbrace{\rho (\varepsilon_{iy} \delta_{jx} + \varepsilon_{jy} \delta_{ix}) \frac{d\bar{u}}{dy}}_{P_{\varepsilon_{xx}}^{(1)}} \\ & \underbrace{-\rho (\varepsilon_{ijxy} + \varepsilon_{ijyx}) \frac{d\bar{u}}{dy}}_{P_{\varepsilon_{ij}}^{(2)}} - \underbrace{\rho \left(2\nu v' \frac{\partial u'_i}{\partial y} \delta_{jx} + 2\nu v' \frac{\partial u'_j}{\partial y} \delta_{ix} \right) \frac{d^2 \bar{u}}{dy^2}}_{P_{\varepsilon_{ij}}^{(3)}} + P_{\varepsilon_{ij}}^{(4)} + \Pi_{\varepsilon_{ij}} - \rho \varepsilon_{\varepsilon_{ij}} = 0 \end{aligned} \quad (\text{A.4})$$

where $\mathcal{E}_{ijk m} := 2\nu \overline{\partial_{x_k} u'_i \partial_{x_m} u'_j}$ (Gerolymos and Vallet, 2016a, (3.1a), p. 402) and the 3 last terms in (A.4) retain their general expressions (1b). The relevant equations for the ε_{ij} -components (recall that by 2-D z -wise symmetry $\varepsilon_{yz}^+ = \varepsilon_{zx}^+ = 0 \forall y^+$) read in wall-units

$$\begin{aligned} & \underbrace{\frac{d}{dy} \left[-\rho \left(\overline{v' 2\nu \frac{\partial u'}{\partial x_k} \frac{\partial u'}{\partial x_k}} \right) \right]}_{d_{\varepsilon_{xx}}^{(u)}} + \underbrace{\mu \frac{d^2 \varepsilon_{xx}}{dy^2}}_{d_{\varepsilon_{xx}}^{(\mu)}} - \underbrace{2\rho \varepsilon_{xy} \frac{d\bar{u}}{dy}}_{P_{\varepsilon_{xx}}^{(1)}} - \underbrace{2\rho \mathcal{E}_{xxxy} \frac{d\bar{u}}{dy}}_{P_{\varepsilon_{xx}}^{(2)}} - \underbrace{4\rho \nu v' \frac{\partial u'}{\partial y} \frac{d^2 \bar{u}}{dy^2}}_{P_{\varepsilon_{xx}}^{(3)}} \\ & + P_{\varepsilon_{xx}}^{(4)} + \Pi_{\varepsilon_{xx}} - \rho \varepsilon_{\varepsilon_{xx}} \stackrel{(\text{A.4})}{=} 0 \end{aligned} \quad (\text{A.5a})$$

$$\begin{aligned} & \underbrace{\frac{d}{dy} \left[-\rho \left(v' 2\nu \frac{\partial u'}{\partial x_k} \frac{\partial v'}{\partial x_k} \right) \right]}_{d_{\varepsilon_{xy}}^{(u)}} + \underbrace{\mu \frac{d^2 \varepsilon_{xy}}{dy^2}}_{d_{\varepsilon_{xy}}^{(\mu)}} \underbrace{-\rho \varepsilon_{yy}}_{P_{\varepsilon_{xy}}^{(1)}} \underbrace{-\rho (\mathcal{E}_{xyxy} + \mathcal{E}_{xyyx})}_{P_{\varepsilon_{xy}}^{(2)}} \frac{d\bar{u}}{dy} \underbrace{-\rho 2\nu v' \frac{\partial v'}{\partial y} \frac{d^2 \bar{u}}{dy^2}}_{P_{\varepsilon_{xy}}^{(3)}} \\ & + P_{\varepsilon_{xy}}^{(4)} + \Pi_{\varepsilon_{xy}} - \rho \varepsilon_{\varepsilon_{xy}} \stackrel{(A.4)}{=} 0 \end{aligned} \quad (A.5b)$$

$$\begin{aligned} & \underbrace{\frac{d}{dy} \left[-\rho \left(v' 2\nu \frac{\partial v'}{\partial x_k} \frac{\partial v'}{\partial x_k} \right) \right]}_{d_{\varepsilon_{yy}}^{(u)}} + \underbrace{\mu \frac{d^2 \varepsilon_{yy}}{dy^2}}_{d_{\varepsilon_{yy}}^{(\mu)}} + \underbrace{0}_{P_{\varepsilon_{yy}}^{(1)}} \underbrace{-2\rho \mathcal{E}_{yyxy}}_{P_{\varepsilon_{yy}}^{(2)}} \frac{d\bar{u}}{dy} + \underbrace{0}_{P_{\varepsilon_{yy}}^{(3)}} \\ & + P_{\varepsilon_{yy}}^{(4)} + \Pi_{\varepsilon_{yy}} - \rho \varepsilon_{\varepsilon_{yy}} \stackrel{(A.4)}{=} 0 \end{aligned} \quad (A.5c)$$

$$\begin{aligned} & \underbrace{\frac{d}{dy} \left[-\rho \left(v' 2\nu \frac{\partial w'}{\partial x_k} \frac{\partial w'}{\partial x_k} \right) \right]}_{d_{\varepsilon_{zz}}^{(u)}} + \underbrace{\mu \frac{d^2 \varepsilon_{zz}}{dy^2}}_{d_{\varepsilon_{zz}}^{(\mu)}} + \underbrace{0}_{P_{\varepsilon_{zz}}^{(1)}} \underbrace{-2\rho \mathcal{E}_{zzxy}}_{P_{\varepsilon_{zz}}^{(2)}} \frac{d\bar{u}}{dy} + \underbrace{0}_{P_{\varepsilon_{zz}}^{(3)}} \\ & + P_{\varepsilon_{zz}}^{(4)} + \Pi_{\varepsilon_{zz}} - \rho \varepsilon_{\varepsilon_{zz}} \stackrel{(A.4)}{=} 0 \end{aligned} \quad (A.5d)$$

where the symmetry relations $\mathcal{E}_{xxxy} = \mathcal{E}_{xyxx}$, $\mathcal{E}_{yyxy} = \mathcal{E}_{yyyx}$ and $\mathcal{E}_{zzxy} = \mathcal{E}_{zzyx}$ were used.

Appendix B. Asymptotic behaviour in the viscous sublayer ($y^+ \rightarrow 0$)

Near a plane xz -wall, located at $y^+ = 0$, the fluctuating quantities are expanded y -wise in Taylor-series around $y^+ = 0$ following (2). The application of the usual gradient-operator (Pope, 2000, (A.48), p. 651) $\nabla(\cdot) := \vec{e}_\ell \partial_{x_\ell}(\cdot)$ on the coefficients of (2), which are stationary random functions of $\{x^+, z^+, t^+\}$ independent of y^+ , produces only in-plane xz -gradients

$$\left(\nabla(\cdot)'_w \right)^+ = \vec{e}_x \frac{\partial(\cdot)'_w^+}{\partial x^+} + \vec{e}_z \frac{\partial(\cdot)'_w^+}{\partial z^+} \quad (B.1a)$$

$$\left(\nabla A'_{(\cdot)} \right)^+ = \vec{e}_x \frac{\partial A'^+_{(\cdot)}}{\partial x^+} + \vec{e}_z \frac{\partial A'^+_{(\cdot)}}{\partial z^+} \quad (B.1b)$$

$$\left(\nabla B'_{(\cdot)} \right)^+ = \vec{e}_x \frac{\partial B'^+_{(\cdot)}}{\partial x^+} + \vec{e}_z \frac{\partial B'^+_{(\cdot)}}{\partial z^+} \quad (B.1c)$$

\vdots

B.1. Fluctuating continuity equation

The no-slip condition (A.1a) implies that the wall-terms in the expansions (2)

$$u'^+_w = v'^+_w = w'^+_w = 0 \quad \forall x^+, z^+, t^+ \quad (B.2)$$

Using the expansions (2), along with (B.2), in the fluctuating continuity equation (Mathieu and Scott, 2000, (4.6), p. 76)

$$\frac{\partial u_\ell'^+}{\partial x_\ell^+} = 0 \quad (\text{B.3})$$

and equating the coefficients of different powers of y^+ to 0, yields

$$A_v'^+ = 0 \quad (\text{B.4a})$$

$$\frac{\partial A_w'^+}{\partial z^+} + \frac{\partial A_u'^+}{\partial x^+} + 2B_v'^+ = 0 \quad (\text{B.4b})$$

$$\frac{\partial B_w'^+}{\partial z^+} + \frac{\partial B_u'^+}{\partial x^+} + 3C_v'^+ = 0 \quad (\text{B.4c})$$

respectively for the $\{O(1), O(y^+), O(y^{+2})\}$ terms, with analogous relations for HOTS. Relation (B.4b) corresponds to Mansour et al. (1988, (3), p. 19). Notice that (B.4b) yields the identity

$$\overline{B_v'^+{}^2} = -\frac{1}{2}\overline{B_v'^+ \frac{\partial A_u'^+}{\partial x^+}} - \frac{1}{2}\overline{B_v'^+ \frac{\partial A_w'^+}{\partial z^+}} \quad (\text{B.5})$$

Relations (2, B.2, B.4, B.5) are generally valid for xz -inhomogeneous incompressible flow near an xz -wall. They provide the wall-asymptotic expansions of all correlations containing only fluctuating velocities and their derivatives, and were used to calculate the wall-asymptotic expansions of $\varepsilon_{\varepsilon_{ij}}$ (Tab. 3) and of its anisotropy tensor $b_{\varepsilon_{\varepsilon_{ij}}}$ and invariants (Tab. 4). The relation of the wall-asymptotic expansion of the fluctuating pressure p' to the expansions of the fluctuating velocities depends on the particular mean-flow studied, and was therefore calculated for fully developed plane channel flow.

B.2. Plane channel flow

In the particular case of plane channel flow, conditions (A.1–A.3) imply specific relations for the mean and fluctuating fields, which were used to determine the wall-asymptotic expansions (Tabs. 1, 2) of various terms in the ε_{ij} -transport (1b) simplified for plane channel flow (A.4, A.5).

B.2.1. Mean-flow Using the expansion of r_{xy}^+ obtained from (2, B.2, B.4a) in the x -wise component of the mean-momentum equation (A.2c) yields, after integration and application of the no-slip boundary-condition (A.1a), the expansion of the mean streamwise velocity

$$\bar{u}^+ \underset{y^+ \rightarrow 0}{\sim} y^+ - \frac{1}{2Re_{\tau_w}} y^{+2} + \frac{1}{4}\overline{A_u'^+ B_v'^+} y^{+4} + \frac{1}{5} \left(\overline{B_u'^+ B_v'^+} + \overline{A_u'^+ C_v'^+} \right) y^{+5} + O(y^{+6}) \quad (\text{B.6a})$$

including the dominant linear term y^+ , an $O(y^{+2})$ correction associated with the mean streamwise pressure-gradient (A.2b), which $\rightarrow 0$ as $Re_{\tau_w} \rightarrow \infty$ at fixed y^+ , and higher $O(y^{+4})$ terms. Therefore, the gradient $[d_y \bar{u}]^+$ and Hessian $[d_{yy}^2 \bar{u}]^+$ which appear in

the production terms $\{P_{\varepsilon_{ij}}^{(1)}, P_{\varepsilon_{ij}}^{(2)}, P_{\varepsilon_{ij}}^{(3)}\}$ of the ε_{ij} -transport equations (1b, A.4, A.5) expand as

$$\frac{d\bar{u}^+}{dy^+} \underset{y^+ \rightarrow 0}{\sim} 1 - \frac{1}{Re_{\tau_w}} y^+ + \overline{A_u'^+ B_v'^+} y^{+3} + \left(\overline{B_u'^+ B_v'^+} + \overline{A_u'^+ C_v'^+} \right) y^{+4} + O(y^{+5}) \quad (\text{B.6b})$$

$$\frac{d^2 \bar{u}^+}{dy^{+2}} \underset{y^+ \rightarrow 0}{\sim} -\frac{1}{Re_{\tau_w}} + 3\overline{A_u'^+ B_v'^+} y^{+2} + 4 \left(\overline{B_u'^+ B_v'^+} + \overline{A_u'^+ C_v'^+} \right) y^{+3} + O(y^{+4}) \quad (\text{B.6c})$$

By (A.2d, 2, B.2, B.4a), the mean pressure can be expanded as

$$\bar{p}^+ \underset{y^+ \rightarrow 0}{\sim} \bar{p}_w^+(x) - \overline{B_v'^+}^2 y^{+4} - 2\overline{B_v'^+ C_v'^+} y^{+5} - (\overline{2B_v'^+ D_v'^+} + \overline{C_v'^+{}^2}) y^{+6} + O(y^{+7}) \quad (\text{B.6d})$$

B.2.2. Wall-normal (y) fluctuating momentum and fluctuating pressure field Using (2, B.2, B.4a, B.6a) in the wall-normal component of the fluctuating momentum equation (Mathieu and Scott, 2000, (4.31), p. 85)

$$\frac{\partial u_i'^+}{\partial t^+} + \bar{u}_\ell^+ \frac{\partial u_i'^+}{\partial x_\ell^+} = -\frac{\partial}{\partial x_\ell^+} (u_i'^+ u_\ell'^+ - r_{i\ell}^+) - u_\ell'^+ \frac{\partial \bar{u}_i^+}{\partial x_\ell^+} - \frac{\partial p'^+}{\partial x_i^+} + \frac{\partial^2 u_i'^+}{\partial x_\ell^+ \partial x_\ell^+} \quad (\text{B.7})$$

and using the symmetry conditions (A.1b) implies that the fluctuating pressure field expansion (2) should be

$$p'^+ \underset{y^+ \rightarrow 0}{\sim} p_w'^+ + 2B_v'^+ y^+ + 3C_v'^+ y^{+2} + \frac{1}{3} \left(12D_v'^+ + (\nabla^2 B_v')^+ - \frac{\partial B_v'^+}{\partial t^+} \right) y^{+3} + \dots \quad (\text{B.8})$$

ie that the fluctuating pressure field, as $y^+ \rightarrow 0$, is uniquely determined to $O(y^{+3})$ by the wall-normal fluctuating velocity field v' (Gerolymos and Vallet, 2016a, (2.3b), p. 391), in line with the plane wall boundary condition $\partial_y p' = \mu \partial_{yy}^2 v'$ (Pope, 2000, (11.173), p. 439). Relation (B.8) corresponds to Mansour et al. (1988, (2, 6), pp. 18–20). In (B.8) $p_w'^+(x^+, z^+, t^+)$ is the fluctuating pressure at the wall.

B.2.3. Wall-parallel (xz) fluctuating momentum Using the expansions (2, B.2, B.4a, B.6) in the fluctuating x -momentum equation (B.7), and equating the coefficients of different powers of y^+ to 0, yields

$$\frac{\partial p_w'^+}{\partial x^+} - 2B_u'^+ = 0 \quad (\text{B.9a})$$

$$2\frac{\partial B_v'^+}{\partial x^+} - \frac{\partial^2 A_u'^+}{\partial z^{+2}} - \frac{\partial^2 A_u'^+}{\partial x^{+2}} + \frac{\partial A_u'^+}{\partial t^+} - 6C_u'^+ = 0 \quad (\text{B.9b})$$

respectively for the $\{O(1), O(y^+)\}$ terms, with the corresponding relations

$$\frac{\partial p_w'^+}{\partial z^+} - 2B_w'^+ = 0 \quad (\text{B.10a})$$

$$2\frac{\partial B_v'^+}{\partial z^+} - \frac{\partial^2 A_w'^+}{\partial z^{+2}} - \frac{\partial^2 A_w'^+}{\partial x^{+2}} + \frac{\partial A_w'^+}{\partial t^+} - 6C_w'^+ = 0 \quad (\text{B.10b})$$

for the fluctuating z -momentum equation (B.7). Relations (B.9a, B.10a) correspond to Mansour et al. (1988, (4), p. 19) and relations (B.9b, B.10b) to Mansour et al. (1988, (7, 8), p. 20).

By (B.9a, B.10a),

$$(B.9a, B.10a) \implies \frac{1}{2} \frac{\partial^2 p_w'^+}{\partial x^+ \partial z^+} = \frac{\partial B_u'^+}{\partial z^+} = \frac{\partial B_w'^+}{\partial x^+} \quad (B.11a)$$

whence, using (A.3a),

$$(B.11a, A.3a) \implies \overline{B_u'^+ \frac{\partial B_w'^+}{\partial x^+}} = \overline{B_w'^+ \frac{\partial B_u'^+}{\partial z^+}} = \overline{B_w'^+ \frac{\partial B_u'^+}{\partial x^+}} = \overline{B_u'^+ \frac{\partial B_w'^+}{\partial z^+}} = 0 \quad (B.11b)$$

Notice that the relations $\overline{B_u'^+ \frac{\partial B_w'^+}{\partial x^+}} \stackrel{(A.3a)}{=} -\overline{B_w'^+ \frac{\partial B_u'^+}{\partial x^+}}$ is also obvious because the flow is 2-D z -wise. Relation (B.11a) corresponds to Mansour et al. (1988, (5), p. 19). Furthermore, substituting $C_v'^+$ by (B.4c) in $\overline{B_u'^+ C_v'^+}$ readily yields by (A.3a, B.11b)

$$\overline{B_u'^+ C_v'^+} \stackrel{(B.4c, A.3a, B.11b)}{=} 0 \quad (B.11c)$$

the corresponding relation $\overline{B_w'^+ C_v'^+} = 0$, which can also be proven in the same way from (B.11b), being obvious because the flow is 2-D in the mean z -wise (A.1b). Finally, by (B.9b, A.3a)

$$\overline{B_v'^+ \frac{\partial A_u'^+}{\partial t^+}} \stackrel{(B.9b, A.3a)}{=} 6 \overline{B_v'^+ C_u'^+} - \frac{\partial A_u'^+}{\partial z^+} \frac{\partial B_v'^+}{\partial z^+} - \frac{\partial A_u'^+}{\partial x^+} \frac{\partial B_v'^+}{\partial x^+} \quad (B.12)$$

References

- Buschmann, M. H. and Gad-el-Hak, M. (2007). Recent developments in scaling of wall-bounded flows, *Prog. Aerosp. Sci.* **42**: 419–467.
- Cécora, R. D., Radespiel, R., Eisfeld, B. and Probst, A. (2015). Differential reynolds-stress modeling for aeronautics, *AIAA J.* **53**: 739–755.
- Chou, P. Y. (1945). On velocity correlations and the solutions of the equations of turbulent fluctuations, *Quart. Appl. Math.* **3**: 38–54.
- Coles, D. (1956). The law of the wake in a turbulent boundary layer, *J. Fluid Mech.* **1**: 191–226.
- Durbin, P. A. (1993). A Reynolds-stress model for near-wall turbulence, *J. Fluid Mech.* **249**: 465–498.
- Eisfeld, B. (ed.) (2015). *Differential Reynolds-stress Modeling for Separating Flows in Industrial Aerodynamics*, Mechanical Engineering Series, Springer, Cham [CHE].
- Gerolymos, G. A. (2011). Approximation error of the Lagrange reconstructing polynomial, *J. Approx. Theory* **163**(2): 267–305.
- Gerolymos, G. A. (2012). A general recurrence relation for the weight-functions in Mühlbach-Neville-Aitken representations with application to WENO interpolation and differentiation, *Appl. Math. Comp.* **219**: 4133–4142.
- Gerolymos, G. A., Joly, S., Mallet, M. and Vallet, I. (2010). Reynolds-stress model flow prediction in aircraft-engine intake double-S-shaped duct, *J. Aircraft* **47**(4): 1368–1381.
- Gerolymos, G. A., Kallas, Y. N. and Papailiou, K. D. (1989). The behaviour of the normal fluctuation terms in the case of attached and detached turbulent boundary-layers, *Rev. Phys. Appl.* **24**(3): 375–387.
- Gerolymos, G. A., Lo, C. and Vallet, I. (2012). Tensorial representations of Reynolds-stress pressure-strain redistribution, *ASME J. Appl. Mech.* **79**(4): 044506(1–10).
- Gerolymos, G. A., Lo, C., Vallet, I. and Younis, B. A. (2012). Term-by-term analysis of near-wall second moment closures, *AIAA J.* **50**(12): 2848–2864.
- Gerolymos, G. A., Sénéchal, D. and Vallet, I. (2009). Very-high-order WENO schemes, *J. Comp. Phys.* **228**: 8481–8524.
- Gerolymos, G. A., Sénéchal, D. and Vallet, I. (2010). Performance of very-high-order upwind schemes for DNS of compressible wall-turbulence, *Int. J. Num. Meth. Fluids* **63**: 769–810.
- Gerolymos, G. A., Sénéchal, D. and Vallet, I. (2013). Wall effects on pressure fluctuations in turbulent channel flow, *J. Fluid Mech.* **720**: 15–65.
- Gerolymos, G. A. and Vallet, I. (2001). Wall-normal-free near-wall Reynolds-stress closure for 3-D compressible separated flows, *AIAA J.* **39**(10): 1833–1842.

- Gerolymos, G. A. and Vallet, I. (2014). Pressure, density, temperature and entropy fluctuations in compressible turbulent plane channel flow, *J. Fluid Mech.* **757**: 701–746.
- Gerolymos, G. A. and Vallet, I. (2016a). The dissipation tensor ε_{ij} in wall turbulence, *J. Fluid Mech.* **807**: 386–418.
- Gerolymos, G. A. and Vallet, I. (2016b). Reynolds-stress model prediction of 3-D duct flows, *Flow Turb. Comb.* **96**(1): 45–93.
- Hoyas, S. and Jiménez, J. (2008). Reynolds number effects on the Reynolds-stress budgets in turbulent channels, *Phys. Fluids* **20**: 101511(1–8).
- Jakirlić, S., Eisfeld, B., Jester-Zürker, R. and Kroll, N. (2007). Near-wall Reynolds-stress model calculations of transonic flow configurations relevant to aircraft aerodynamics, *Int. J. Heat Fluid Flow* **28**: 602–615.
- Jakirlić, S. and Hanjalić, K. (2002). A new approach to modelling near-wall turbulence energy and stress dissipation, *J. Fluid Mech.* **459**: 139–166.
- Jakirlić, S. and Hanjalić, K. (2013). A DNS-based reexamination of coefficients in the pressure-strain models in second-moment closures, *Fluid Dyn. Res.* **45**: 055509(1–22).
- Jones, W. P. and Launder, B. E. (1972). The prediction of laminarization with a 2-equation model of turbulence, *Int. J. Heat Mass Transfer* **15**: 301–314.
- Kassinos, S. C., Reynolds, W. C. and Rogers, M. M. (2001). 1-point turbulence structure tensors, *J. Fluid Mech.* **428**: 213–248.
- Lai, Y. G. and So, R. M. C. (1990). On near-wall turbulent flow modelling, *J. Fluid Mech.* **221**: 641–673.
- Launder, B. E., Reece, G. J. and Rodi, W. (1975). Progress in the development of a Reynolds-stress turbulence closure, *J. Fluid Mech.* **68**: 537–566.
- Launder, B. E. and Spalding, D. B. (1974). The numerical computation of turbulent flows, *Comp. Meth. Appl. Mech. Eng.* **3**: 269–289.
- Lee, M. J. and Reynolds, W. C. (1987). On the structure of homogeneous turbulence, in F. Durst, B. E. Launder, J. L. Lumley, F. W. Schmidt and J. H. Whitelaw (eds), *Turbulent Shear Flows 5, Selected Papers for the 5. International Symposium on Turbulent Shear Flows, Cornell University, Ithaca [NY, USA], aug, 7–9, 1985*, Springer, Berlin [DEU], pp. 54–66.
- Lee, M. and Moser, R. D. (2015). DNS of turbulent channel flow up to $Re_\tau \approx 5200$, *J. Fluid Mech.* **774**: 395–415.
- Lumley, J. L. (1978). Computational modeling of turbulent flows, *Adv. Appl. Mech.* **18**: 123–176.
- Lumley, J. L., Yang, Z. and Shih, T. H. (1999). A length-scale equation, *Flow Turb. Comb.* **63**: 1–21.
- Mansour, N. N., Kim, J. and Moin, P. (1988). Reynolds-stress and dissipation-rate budgets in a turbulent channel flow, *J. Fluid Mech.* **194**: 15–44.
- Mathieu, J. and Scott, J. (2000). *An introduction to turbulent flow*, Cambridge University Press, Cambridge [GBR].
- Menter, F. R. (1994). 2-equation eddy-viscosity turbulence models for engineering applications, *AIAA J.* **32**(8): 1598–1605.
- Monin, A. S. and Yaglom, A. M. (1971). *Statistical fluid mechanics: Mechanics of turbulence*, Vol. 1, MIT Press, Cambridge [MA, USA].
- Moser, R. D., Kim, J. and Mansour, N. N. (1999). Direct numerical simulation of turbulent channel flow up to $Re_\tau = 590$, *Phys. Fluids* **11**(4): 943–945.
URL: <http://www.turbulence.ices.utexas.edu/>
- Olsen, M. E. and Coakley, T. J. (2001). The lag model, a turbulence model for nonequilibrium flows, AIAA Paper 2001–2564.
- Pope, S. B. (2000). *Turbulent Flows*, Cambridge University Press, Cambridge [GBR].
- Riley, K. F., Hobson, M. P. and Bence, S. J. (2006). *Mathematical Methods for Physics and Engineering*, 3 edn, Cambridge University Press, Cambridge [GBR].
- Rivlin, R. S. (1955). Further remarks on the stress-deformation relations for isotropic materials, *Indiana Univ. Math. J.* **4**: 681–702.
- Rodi, W. and Mansour, N. N. (1993). Low Reynolds number $k-\varepsilon$ modelling with the aid of DNS, *J. Fluid Mech.* **250**: 509–529.
- Rumsey, C. L. (2010). NASA Langley Research Center Turbulence Modeling Resource, <http://turbmodels.larc.nasa.gov/index.html>, visited nov 2014.
- Schiestel, R. (2008). *Modelling and Simulation of Turbulent Flows*, ISTE John Wiley and Sons, London [GBR].
- Schultz, M. P. and Flack, K. A. (2013). Reynolds-number scaling of turbulent channel flow, *Phys. Fluids* **25**: 025104(1–13).
- Sillero, J. A., Jiménez, J. and Moser, R. D. (2013). One-point statistics for turbulent wall-bounded flows at Reynolds numbers up to $\delta^+ \approx 2000$, *Phys. Fluids* **25**: 105102(1–16).

- Simonsen, A. J. and Krogstad, P. Å. (2005). Turbulent stress invariant analysis: Classification of existing terminology, *Phys. Fluids* **17**: 088103(1–4).
- Speziale, C. G., Sarkar, S. and Gatski, T. B. (1991). Modelling the pressure-strain correlation of turbulence: An invariant dynamical systems approach, *J. Fluid Mech.* **227**: 245–272.
- Tennekes, H. and Lumley, J. L. (1972). *A First Course in Turbulence*, MIT Press, Cambridge [MA, USA].
- Vreman, A. W. and Kuerten, J. G. M. (2014a). Comparison of DNS databases of turbulent channel flow at $Re_\tau = 180$, *Phys. Fluids* **26**: 015102(1–21).
- Vreman, A. W. and Kuerten, J. G. M. (2014b). Statistics of spatial derivatives of velocity and pressure in turbulent channel flow, *Phys. Fluids* **26**: 085103(1–29).
- Vreman, A. W. and Kuerten, J. G. M. (2016). A 3-order multistep time-discretization for a chebyshev tau spectral method, *J. Comp. Phys.* **304**: 162–169.
- Wilcox, D. C. (1988). Reassessment of the scale-determining equation for advanced turbulence models, *AIAA J.* **26**: 1299–1310.
- Wilcox, D. C. (2006). *Turbulence Modelling for CFD*, 3. edn, DCW Industries, La Cañada [CA, USA].
- Yakovenko, S. N. and Chang, K. C. (2007). Performance examination of geometry-independent near-wall second-moment closures in simple and backstep flows, *Num. Heat Transfer B* **51**(2): 179–204.
- Zanoun, E. S., Nagig, H. and Durst, F. (2009). Refined c_f relation for turbulent channels and consequences for high- Re experiments, *Fluid Dyn. Res.* **41**: 021405(1–12).